NASA/CR-2002-211918

Characterizing the Severe Turbulence Environments Associated With Commercial Aviation Accidents

Part I: 44 Case Study Synoptic Observational Analyses

Michael L. Kaplan, Allan W. Huffman, and Kevin M. Lux
North Carolina State University, Raleigh, North Carolina

Joseph J. Charney
North Central Research Station, East Lansing, Michigan

Allan J. Riordan and Yuh-Lang Lin
North Carolina State University, Raleigh, North Carolina

August 2002

The NASA STI Program Office . . . in Profile

Since its founding, NASA has been dedicated to the advancement of aeronautics and space science. The NASA Scientific and Technical Information (STI) Program Office plays a key part in helping NASA maintain this important role.

The NASA STI Program Office is operated by Langley Research Center, the lead center for NASA's scientific and technical information. The NASA STI Program Office provides access to the NASA STI Database, the largest collection of aeronautical and space science STI in the world. The Program Office is also NASA's institutional mechanism for disseminating the results of its research and development activities. These results are published by NASA in the NASA STI Report Series, which includes the following report types:

- TECHNICAL PUBLICATION. Reports of completed research or a major significant phase of research that present the results of NASA programs and include extensive data or theoretical analysis. Includes compilations of significant scientific and technical data and information deemed to be of continuing reference value. NASA counterpart of peer-reviewed formal professional papers, but having less stringent limitations on manuscript length and extent of graphic presentations.

- TECHNICAL MEMORANDUM. Scientific and technical findings that are preliminary or of specialized interest, e.g., quick release reports, working papers, and bibliographies that contain minimal annotation. Does not contain extensive analysis.

- CONTRACTOR REPORT. Scientific and technical findings by NASA-sponsored contractors and grantees.

- CONFERENCE PUBLICATION. Collected papers from scientific and technical conferences, symposia, seminars, or other meetings sponsored or co-sponsored by NASA.

- SPECIAL PUBLICATION. Scientific, technical, or historical information from NASA programs, projects, and missions, often concerned with subjects having substantial public interest.

TECHNICAL TRANSLATION. English-language translations of foreign scientific and technical material pertinent to NASA's mission.

Specialized services that complement the STI Program Office's diverse offerings include creating custom thesauri, building customized databases, organizing and publishing research results . . . even providing videos.

For more information about the NASA STI Program Office, see the following:

- Access the NASA STI Program Home Page at ***http://www.sti.nasa.gov***

- Email your question via the Internet to help@sti.nasa.gov

- Fax your question to the NASA STI Help Desk at (301) 621-0134

- Telephone the NASA STI Help Desk at (301) 621-0390

- Write to:
  NASA STI Help Desk
  NASA Center for AeroSpace Information
  7121 Standard Drive
  Hanover, MD 21076-1320

NASA/CR-2002-211918

Characterizing the Severe Turbulence Environments Associated With Commercial Aviation Accidents

Part I: 44 Case Study Synoptic Observational Analyses

Michael L. Kaplan, Allan W. Huffman, and Kevin M. Lux
North Carolina State University, Raleigh, North Carolina

Joseph J. Charney
North Central Research Station, East Lansing, Michigan

Allan J. Riordan and Yuh-Lang Lin
North Carolina State University, Raleigh, North Carolina

National Aeronautics and
Space Administration

Langley Research Center
Hampton, Virginia 23681-2199

Prepared for Langley Research Center
under Contract NAS1-99074

August 2002

Acknowledgments

This research was supported by the NASA Langley Research Center under contract NAS1-99074 and subcontract 82U-7473-008 to the Research Triangle Institute. The authors wish to thank Dr. Fred H. Proctor, the NASA Technical Contract Manager, for his support.

Available from:

NASA Center for AeroSpace Information (CASI)
7121 Standard Drive
Hanover, MD 21076-1320
(301) 621-0390

National Technical Information Service (NTIS)
5285 Port Royal Road
Springfield, VA 22161-2171
(703) 605-6000

Table of Contents

List of Tables

List of Figures

Summary

This paper describes the results of a 44 case study analysis of the large-scale atmospheric structure associated with development of accident-producing aircraft turbulence. First, the 44 cases are categorized as a function of the accident location, altitude, time of year, time of day, and the turbulence category, which classifies a disturbance as in clear air, in-cloud, in convection, near mountains, or near but not in deep convection. It is noteworthy that cases fell more frequently in this latter category than was initially anticipated. Second, National Centers for Environmental Prediction Reanalyses data sets and satellite imagery are employed to diagnose synoptic scale "predictor" fields associated with the large-scale environment preceding severe turbulence.

The results of these analyses indicate a predominance of severe accident-producing turbulence within the entrance region of a jet stream at the synoptic scale. Typically, there is a region of flow curvature just upstream within the jet entrance region, convection is within 100 km of the accident, vertical motion is upward, absolute vorticity is low, vertical wind shear is increasing, and horizontal cold advection is substantial. The most consistent predictor is upstream curvature in the flow. Nearby convection is the second most frequent predictor.

1. Introduction

Turbulence is an extraordinarily challenging subject long studied by engineers, computational fluid dynamics experts, and atmospheric scientists. It is of critical interest to aviators because of the significant impact it can have on aircraft. According to a 1998 press release from the U.S. Department of Transportation, in-flight turbulence is the leading cause of nonfatal accidents to airline passengers and flight attendants. Major airlines reported 252 incidents of turbulence that resulted in 2 deaths, 63 serious injuries, and 863 minor injuries from 1981–1996. Pilots generally do not know when severe turbulence will occur because there is little warning from meteorologists. Turbulence is extremely difficult to predict due to the fact it often occurs in a microscale environment, usually from hundreds of square meters to 1 to 2 km^2 in area.

Previous studies of synoptic environments producing turbulence have shown that turbulence can occur near upper level frontal zones (Reed and Hardy 1972), near mountains (Lilly and Zipser 1972; Clark et al. 2000), and in clear air (CAT) (Chambers 1955). Turbulence can also occur in and near convection due to the violent, rapidly changing upward and downward motions, and due to gravity waves that can form in and around the convection (Kaplan et al. 1997; 2000). Roach (1970) and Reed and Hardy (1972) showed that the confluence of two different flow fields in the entrance region of a jet stream is conducive to turbulence generation. Uccellini et al. (1986) showed, through observations and numerical model simulations, that at the time of the Space Shuttle Challenger accident the polar jet (PJ) and the subtropical jet (STJ) were juxtaposed over the launch site, a condition that can produce very large vertical wind shears. Endlich (1964), Reiter and Nania (1964), Mancuso and Endlich (1966), Keller (1990), and Ellrod and Knapp (1992) focused on the possible relationship between frontogenesis, jet streams, wind shear, and CAT. Ellrod and Knapp (1992) observed that much of the significant CAT in their data occurred where the total deformation and vertical wind shear were both relatively large. They formulated an equation relating vertical wind shear and deformation:

$$TI1 = VWS \times DEF \quad (1)$$

where VWS = vertical wind shear and DEF = total deformation. Both these values, in units of s^{-2}, were obtained from u and v components produced by numerical forecast models from the National Meteorological Center. Knox (1997) examined CAT in regions of strong anticyclonic flow. He argued that the linkage between frontogenesis, deformation, and CAT is not appropriate in anticyclonic flows and that the CAT generated in anticyclonic flow is not accounted for in conventional CAT theory. He suggested that geostrophic adjustment and inertial

instability, especially in strongly anticyclonic flows, could cause CAT. He proposed that future CAT indices should include inertial instability and geostrophic adjustment in their formulations. Existing operational turbulence forecasting algorithms, such as those developed by Marroquin (1998), Marroquin et al. (1998), and Sharman, Wiener, and Brown (2000), are designed to provide forecast guidance for a spectrum of turbulence intensities from light to severe.

This three-part sequence of papers differs from the aforementioned studies in that the focus is restricted to severe accident-producing aircraft turbulence. An accident in this study indicates an event during which injuries occurred to passengers and/or crew as a result of severe turbulence. It is important to emphasize the element of surprise as severe turbulence is totally unexpected; as such, little could be done to prevent injuries to passengers or crew. By analyzing accident-producing case studies we strive to develop better forecasting products for prediction of this hazard to commercial aviation. Furthermore, as part of this process, we plan to synthesize the sequence of dynamical adjustments that lead to violent turbulence into a paradigm that is consistently useful in understanding when and where severe turbulence will occur.

In Part I of this study, an observational analysis of the synoptic scale meteorological conditions present in 44 cases of reported severe accident-producing turbulence is performed. The common dynamic signals in these cases are examined and a paradigm of the most prevalent atmospheric conditions is formulated. The purpose is to provide a foundation for the mesoscale and microscale simulation studies to be presented in Parts II and III, in other words, to provide coarse but highly persistent and reproducible evidence of the synoptic state of the atmosphere prior to severe turbulence events. When coupled with the very high-resolution simulation studies in Parts II and III, a paradigm will emerge forming the groundwork for development of an improved severe turbulence potential forecast product.

In the following section, the process by which data for the 44 cases were obtained is given, the way in which individual cases were classified is discussed, and background information for the cases is provided. Section 3 discusses how the data were processed and the common synoptic meteorological signals detected. Section 4 describes several specific case study examples of the primary common synoptic observational features in the accident-producing turbulence case studies. Finally, section 5 presents a summary in the form of a synoptic scale paradigm that serves as a logical precursor to the mesoscale and microscale issues to be discussed in Parts II and III.

2. Forty-Four Case Study Categorization

2.1. Data Description

Classification data for 44 cases of severe turbulence, i.e., wherein commercial aircraft encountered severe turbulence and onboard injuries occurred, were obtained from the National Transportation Safety Board (NTSB) archive of aviation accident narratives. These case studies occurred from 1990–1996 and the list of cases was provided by NASA Ames Research Center. Also included were the date, approximate location of the turbulence, time, height, and the probable class/cause of the turbulence. The classes of turbulence were sorted into four categories: clear air turbulence (CAT), mountain (MTN), thunderstorm (TRW), and cloud (CLD). However, the only information about weather included in the NASA analysis was the surface aviation station observation at the hourly time period closest to the accident. This obviously falls short of a comprehensive synoptic scale analysis; therefore, in order to thoroughly diagnose the synoptic regime present for these cases, National Centers for Environmental Prediction (NCEP) Global Reanalyses data sets (Kalnay et al. 1996) were obtained for all 44 cases. The reanalysis data consisted of six hourly data sets of temperature, height, wind, and mixing ratio on constant

pressure surfaces across the globe. The data constitute observations from rawinsondes, profilers, satellite, radar, and surface observations assimilated onto a grid of 2.5° horizontal resolution for all mandatory levels. The graphical analysis was done using GEMPAK 5.4. Also to aid in our analysis, NOAA NESDIS-derived high-resolution 1-km visible and 4-km infrared satellite imagery were used. This was available for 43 of the 44 case studies and was useful in determining the type and distribution of clouds for the cases.

2.2. Further Classification of Turbulence Categories

After performing an in-depth analysis of satellite data associated with the 44 cases, it became obvious that the classification of turbulence was incomplete. There were several case studies wherein the turbulence occurred in proximity to but not directly within ongoing deep convection, like that of a thunderstorm. This situation occurred because pilots generally attempt to circumnavigate deep convection, but often the violent turbulence was reported immediately after a pilot had passed by the convection. A new category was therefore created to describe thunderstorm conditions that occurred in proximity to the aircraft and that were accompanied by severe turbulence when the aircraft was clearly not in the convective cells. In other words, the pilots had to report sitings of convection even though turbulence occurred after the aircraft was out of convective clouds. (It should be noted that in this instance we are describing deep convection with at least a level one intensity on radar. In a more general sense, convection was ubiquitous in these case studies even when the bases were in the middle and upper troposphere, unlike typical thunderstorms.) This new category was named TRW* for convective storms within a reasonable view of the cockpit and noted by the pilot, but with turbulence occurring outside of the convection. An example of TRW* can be seen for a case of turbulence near South Bend, Indiana, that occurred at 2159 UTC 7 July 1994. Figure 1(a) shows the NTSB narrative for the incident and figure 1(b) shows the GOES visible satellite imagery of the accident location near South Bend at 2201 UTC 7 July 1994. Upon examining the NTSB report, one finds the pilot did not mention flying directly in convection within the area and therefore NASA personnel classified this case as CAT. It is apparent, however, that widespread convection existed very close to South Bend, and the pilot did note that radar was used to avoid weather, the implication being that the pilot was near but not within deep convection at the time of the accident.

The addition of the TRW* category led to a change in breakdown of the probable causes of turbulence for all the case studies. Table 1 shows the numeric distribution of weather categories for the 44 cases based on the original NASA classification. Table 2 depicts the numerical redistribution of case studies from their original classifications to the TRW* category. (Note that the TRW* category constitutes 13 of the 44 cases and is the second largest classification.) Additional analysis using satellite imagery showed that nine of the cases that remained classified CAT and two that remained classified as MTN were actually within 30 km of deep convection although no convection was noted in pilot reports. These cases were not added to the TRW* category because the pilot noted no convection; nevertheless, this seemed to indicate that proximity to convection was an important consideration. Additionally, the 44 case studies were categorized as a function of geographical region, time of year, time of day, and altitude. The findings include the following:

(1) The location where severe turbulence was most often encountered was the southeastern U.S., followed by the south-central U.S. and the tropical oceanic regions, all of which account for more than half of the total (table 3).

(2) The time of year most common was the warm season—more than 40 percent of case studies occurred in summer—with June and July having the most frequent occurrences and the combined spring and summer period accounting for more than 70 percent of the total (table 4).

(3) The preferred time of day was between 1700 and 0000 UTC, wherein more than half the case studies occurred (table 5).

(4) The preferred altitude (not including case studies reported as descent, final approach, or climb out) was between 9 and 12 km with close to 40 percent of case studies lying in this range; the 6 to 9 km range accounted for nearly half the remaining case studies, and an average elevation of ~7300 m existed for all case studies (table 6).

(5) TRW* case studies were more numerous than TRWs and nearly as numerous as CATs, a finding consistent with the first four. All findings highlight the importance of convection, which was within 100 km of turbulence in 86 percent of the case studies (table 10). Proximity to convection was likely more important than existence of a very strong jet stream, which occurred in a minority of case studies. Typically the jet stream was in proximity to the accident but was not notably strong.

3. Diagnosis of the Synoptic Paradigm

3.1. Calculation of the Synoptic Predictor Fields

In an effort to determine the most prevalent synoptic scale atmospheric configuration associated with severe turbulence reports, nearly two dozen predictor fields from the NCEP Reanalyses data sets and the corresponding satellite images were calculated. By predictor fields it is meant those fields unambiguously associated with the location and time of a turbulence accident event. Predictor fields were composed of kinematical, dynamical, and thermodynamic fields, i.e., dependent variables or vertical wind shear, static stability, vorticity, divergence, and vertical motions, etc. (table 9). Calculating the predictor fields technically meant diagnosing whether or not these specific dynamical fields tended to be large or small in magnitude, or in a certain configuration when and where severe turbulence occurred. The diagnostic process therefore aided in determining the relative utility of predictor fields in forecasting turbulence. By doing this for many different dependent variables and derived fields, a synoptic model of the environment favored for severe accident-producing turbulence could be built. No in-depth statistical analyses were performed employing these predictor fields due to the small sample size of case studies belonging to each category of turbulence. Since in-depth statistical analyses were not possible, the predictor status is intended to suggest association based on proximity.

Calculations of the predictor fields were performed at the 6-hourly NCEP Reanalyses data sets time and satellite imagery time (typically within 4 to 8 minutes) closest to the NTSB data base's reported time of the accident. The predictor fields were ascertained at the constant pressure level closest to the altitude of the accident and centered in space on the location of the accident. Horizontal and vertical cross sections were constructed and the closest available analyses/satellite data time used in an effort to derive predictors centered in three-dimensional space. Vertical cross sections were calculated both along and normal to the jet stream, centered on the accident location, and agreed tangentially to the flight path of each accident from origination to destination. Tables 7 through 9 depict lists of these horizontal and vertical cross section fields as well as the specific predictor fields.

3.2. Primary Signals in the Synoptic Predictor Fields

The synoptic predictor fields depicted in table 9 represent standard derived quantities often associated with turbulence in meteorological literature (e.g., Keller 1990; Ellrod and Knapp 1992; Knox 1997). These predictor fields were calculated and then the magnitudes compared to location, elevation, and time of the accident. From these comparisons, we were able to derive simple numerical indicators of the most and least useful predictor fields for determining when and where

severe accident-producing turbulence should be occurring. Table 10 shows the five most meaningful predictors from all case studies based on their proximity in space and time to the accidents:

(1) Upstream trough/ridge axis in the height field at a distance of less than 500 km (occurring in 43 of the 44 cases)

(2) Convection less than 100 km away (occurring in 38 of the 44 cases) and at the accident site

(3) Upward vertical motion

(4) Layer-averaged absolute vorticity $\leq 10^{-4}$ s^{-1}

(5) Jet stream entrance region (occurring in 34 of the 44 cases)

While there are slight variations for each individual category of turbulence, as depicted in tables 11 through 15, the most persistent signals across the various categories are a ridge or trough axis and hence a region of changing flow curvature, convection, upward vertical motion, low relative vorticity, the entrance region of a jet stream, and horizontal cold advection.

4. Synoptic Signals in Individual Case Studies

This section of the paper briefly describes seven case study examples from several categories, including TRW*, TRW, CAT, and CLD, that indicate the preferred synoptic regime for severe turbulence and emphasize the redundancy of many synoptic predictor fields. As can be seen from table 10, many of the studies share all or a majority of the key characteristics that will be described. Therefore, these seven studies are highly representative of the majority of cases as they all occur within a curved flow regime, within the entrance region of a jet stream, with upward vertical motion, low relative vorticity, cold air advection, and nearby convection. All occurred relatively close to a minimum value of the vertical variation of the Richardson number, although coarse, three-dimensional resolution of the data produced Richardson number values that varied considerably and were relatively large in magnitude. We will also examine a case that violated this paradigm and discuss common factors that served as significant outliers in approximately 20 to 25 percent studies.

4.1. South Bend, Indiana—TRW*, July 7, 1994

Figure 1 describes the NTSB narrative for this accident event, indicating nearby convection, but includes no pilot report of being in a convective cell during the turbulence incident, which occurred between 500 and 400 mb. Other key fields are depicted in figure 2, illustrating a 500 mb flow regime in which a moderately strong jet core was located over Quebec with the accident location in the right entrance region of that jet core. The ageostrophic flow was directed toward the left and there was a definite anticyclonic to cyclonic variation in flow curvature. Absolute vorticity values were less than the Coriolis parameter, indicating negative relative vorticity. An along-stream variation of ascent indicated the curved structure of the flow with the accident site still in the upward motion at the time of the observations. Additionally, weak cold advection was occurring near and just upstream of the accident location. There was no relative Richardson number minimum near the level of the accident.

4.2. Alma, Georgia—CAT, March 16, 1995

While this was categorized as a CAT case study because the pilot did not mention nearby convection (fig. 3(a)), deep convective cells were obviously near the aircraft's flight path as can be seen from the satellite image in figure 3(b). Figure 4 indicates that the accident occurred within the left entrance region of a moderately strong ~200 mb jet stream centered over southern Florida. The ageostrophic flow was leftward directed and there was neutral-weak cold advection. Substantial flow curvature existed as

the accident location was between a relatively short wavelength ridge to the east and a trough upstream, and within the upward motion region. Absolute vorticity values were slightly larger than the Coriolis parameter, indicating that the left entrance region was not a locus of large cyclonic vorticity, that is, the vorticity maximum was more closely aligned with the cyclonic curvature just upstream. There was no relative Richardson number minimum near the level of the accident.

4.3. Granite, Colorado—CAT, June 22, 1996

This case study occurred near 400 mb in proximity to deep convection. However, as in the previous case study, the pilot's not mentioning or reporting the presence of convection caused it to be classified as CAT (fig. 5). The accident occurs in the right entrance region of a moderately strong jet stream as is depicted in figure 6. The upstream flow curvature is significant. The ageostrophic flow is directed slightly to the left, the absolute vorticity is approximately equivalent to the Coriolis parameter, there is cold advection, and the vertical motion is in the transition zone from sinking to rising motion at the synoptic scale. However, the multiple convective cells imply numerous subsynoptic scale ascent regions. The Richardson number was low through a deep layer including the accident level.

4.4. Miami, Florida—TRW, July 14, 1990

This event occurred within deep convection (fig. 7) at a relatively low elevation of ~4000 m. A weak jet core was centered to the northeast of Florida with its right entrance region over Miami (fig. 8(a)). Strong curvature existed just south of the accident location wherein upward vertical motion and cold advection were occurring. Absolute vorticity values were considerably less than the Coriolis parameter, indicating negative relative vorticity. The ageostrophic flow was again leftward directed. A relative Richardson number minimum was observed near the accident elevation.

4.5. Fort Myers, Florida—CAT, July 18, 1990

In this event no mention of convection was found in the NTSB narrative; thus, it remained a CAT case study even though the aircraft was very close to deep convection, as can be seen in figure 9. The 300 mb winds (fig. 10) indicate two jet streams, a moderately strong westerly wind maximum over the Carolinas and a weak easterly maximum over the Bahamas. Fort Myers was located in the right entrance region of the northernmost stream. A comparison with the flow at 200 mb (not shown) indicates that the accident level was in the transition zone from a dominance of the westerly stream to the easterly stream at ~250 mb. The curvature maximum was again just south of the accident location and the vorticity was considerably less than the Coriolis parameter in magnitude. Ageostrophic flow was directed toward the jet and into the jet entrance region. Weak cold advection and upward vertical motion were both occurring in the accident location. A relative Richardson number minimum was observed at the accident location.

4.6. East Hampton, New York—TRW, June 29, 1994

In this case study, the aircraft was in-cloud and there were nearby thunderstorms. It was very hard to decipher exactly where the aircraft was relative to convection at the time of severe turbulence (based on the narrative provided in fig. 11). The satellite imagery indicates abundant nearby convection. The event occurred on the right flank of and very close to the entrance region of a moderately strong 300 mb jet stream centered north of the accident location with leftward-directed ageostrophic flow (fig. 12). There was a pronounced upstream curvature maximum with strong cold advection, upward vertical motion, and absolute vorticity much less than the Coriolis parameter. A relative minimum in the Richardson number could be found just below the accident location.

4.7. Grand Rapids, Michigan—TRW*, August 4, 1995

In this case study, while the pilot reported no convection, weather logs of the airline indicated that convection was nearby during the turbulence event, as can be seen in figure 13(a). The satellite imagery indicated convection very close to the accident location (fig. 13(b)). It occurred just below 300 mb where a fairly weak jet core was located over the northern Great Lakes and south-central Canada (fig. 14(a)). The accident occurred in the right entrance region of the stream with leftward-directed ageostrophic flow. Cold advection, upward vertical motion, and very low absolute vorticity existed where the accident was reported. Curvature was weaker than most case studies but still existed upstream. A relative minimum of Richardson number could be found at the level of the accident.

4.8. Counterpoint Case Studies

While approximately 75 to 80 percent of the 44 case studies closely share the aforementioned dynamical characteristics, for the remaining ~20 to 25 percent, many aspects of the synoptic environment differ. These anomalies are found for all five categories of turbulence; an example of such an anomaly is seen in figure 15. A TRW-category case study accident occurred near Buffalo, New York, on March 23, 1991 at ~250 mb. Nothing about this case study conforms to the previous seven studies except that there were significant curvature and cold advection. This accident occurred in the left exit region of a highly curved jet stream with sinking motion and rightward-directed ageostrophic flow. Accidents in the right entrance region with ascending leftward-directed ageostrophic flow were much more typical. Further, the vorticity is much greater than the Coriolis parameter rather than less as was the case in the previous seven studies and the majority of other cases. Finally, there is no obvious relative minimum in the vertical profile of the Richardson number. Only a few of these 10 anomalous cases differ so drastically from the 34 others. In fact, all but two of the ten cases have significant cold advection, all but one have a highly curved jet stream, and all but seven have very low absolute vorticity.

One could infer that when the classic jet stream structure—entrance region location of the accident, upward vertical motion, or low vorticity—is missing, the cold advection and curvature increase considerably. The inference is that *some combination of curvature and solenoidal/cold frontal structure is the key to understanding what establishes an environment predisposed to turbulence.* The paradigm seems strongly weighted toward inertial-advective adjustments in a baroclinic zone. Hence, ageostrophic frontogenetical processes are likely important in the turbulence accident environment. This clearly indicates, however, that signals at the synoptic scale are only a partial indicator of the possibility of severe turbulence and that mesoscale and microscale processes may refine the probability of how favorable or unfavorable a synoptic environment will be for producing turbulence. Additional research may very well yield a mesoscale and/or microscale synthesis that distills the common signals among all 44 case studies.

5. Summary and Discussion

Part I of this study has shown that atmospheric, geographical, and seasonal commonalities were observed in 44 cases of severe turbulence. NCEP Reanalyses data were obtained for all case studies and used in the analysis. The data indicate that for these cases, the most common time and location for severe turbulence to occur were in the summer at a flight level between 9000 and 12 000 m across the southeastern United States. Also, by using satellite imagery to aid in our analysis, it was determined that convection played a key role in the severe turbulence reports in this data set with a majority of the cases (86 percent) occurring within 100 km of moist convection. It was also shown that the most important synoptic signals pointed to an environment where convection coincided with a curved jet stream entrance region, upward vertical motions, low relative vorticity, horizontal cold advection, and

leftward-directed ageostrophic flow. Increasing vertical wind shear with time was a rather common feature as well. It was also apparent that relative minimum values of Richardson number calculated from synoptic scale observations are not well-correlated with incidents of turbulence, probably due to the lack of vertical detail in the observational data sets. In addition, the strength of the jet stream was less clearly associated with turbulence accidents than were the convection and the jet's curvature. These features were relatively similar in all five categories of turbulence. When all five features, or predictors, were not present, strong signals of curvature and cold advection were still evident, indicating that these two processes or their effects on the mesoscale and microscale environments somehow are critical to the development of turbulence. The synoptic evidence points toward the juxtapositioning of inertial-advective forcing (large horizontal curvature and low vertical vorticity) and cold air advection in an environment that supports moist convection. This type of environment would be favored by a confluent jet entrance region or regions where curved flow supports highly ageostrophic ascending motions and moist convection.

One of the important conclusions of this study is that a relatively small number of the events were actually associated with CAT.

In Parts II and III of this study, these findings will be compared with four additional cases of severe accident-producing turbulence including convective and clear-air case studies. All four of these case studies share the same synoptic signals described in the present research. The analysis in Parts II and III will focus on a much smaller scale by examining the meso-beta and meso-gamma scale signals derived from numerical simulations for the accident sites of these four cases.

6. References

Chambers, E. 1955: Clear Air Turbulence and Civil Jet Operation. *J. Roy. Aeronaut. Soc.*, **59**, 613–628.

Clark, T. L.; Hall, W. D.; Kerr, R. M.; Middleton, D.; Radke, L.; Martin, Ralph F.; Nieman, P. J.; and Levinson, D. 2000: Origins of Aircraft-Damaging Clear Air Turbulence During the 9 December 1992 Colorado Downslope Windstorm: Numerical Simulations and Comparison to Observations. *J. Atmos. Sci.*, **57**, 1105–1131.

Ellrod, G. P.; and Knapp, D. I. 1992: An Objective Clear-Air Turbulence Forecasting Technique: Verification and Operational Use. *Wea. Forecasting*, **7**, 150–165.

Endlich, R. M. 1964: The Mesoscale Structure of Some Regions of Clear-Air Turbulence. *J. Appl. Meteor.*, **3**, 261–276.

Kalnay, E., et al. 1996: The NMC/NCAR 40-year Reanalysis Project. *Bull. Amer. Meteor. Soc.*, **77**, No. 3, 437–471.

Kaplan, M. L.; Koch, S. E.; Lin, Y-L.; Weglarz, R. P.; and Rozumalski, R. A. 1997: Numerical Simulations of a Gravity Wave Event Over CCOPE. Part I: The Role of Geostrophic Adjustment in Mesoscale Jetlet Formation. *Mon. Wea. Rev.*, **125**, 1185–1211.

Kaplan, M. L.; Lin, Y-L.; Riordan, A. J.; Lux, K. M.; and Huffman, A. W. 2000: Observational and Numerical Simulation-Derived Factors That Characterize Turbulence Accident Environments. Preprints, *9th AMS Conference on Aerospace, Range, and Aeronautical Meteorology*, 11–15 September 2000, 476–481.

Keller, J. L. 1990: Clear-Air Turbulence as a Response to Meso- and Synoptic-Scale Dynamical Processes. *Mon. Wea. Rev.*, **118**, 2228–2242.

Knox, J. A. 1997: Possible Mechanisms of Clear-Air Turbulence in Strongly Anticyclonic Flows. *Mon. Wea. Rev.*, **125**, 1251–1259.

Lilly, D. K.; and Zipser, E. J. 1972: The Front Range Windstorm of 11 January 1972: A Meteorological Narrative. *Weatherwise*, **25**, 56–63.

Mancuso, R. L.; and Endlich, R. M. 1966: Clear-Air Turbulence Frequency as a Function of Wind Shear and Deformation. *Mon. Wea. Rev.*, **94**, 581–585.

Marroquin, A. 1998: An Advanced Algorithm To Diagnose Atmospheric Turbulence Using Numerical Model Output. Preprints, *16th AMS Conference on Weather Analysis and Forecasting*, 11–16 January 1998, 79–81.

Marroquin, A.; Smirnova, T. G.; Brown, J. M.; and Benjamin, S. G. 1998: J4.7 Forecast Performance of a Prognostic Turbulence Formulation Implemented in the MAPS/RUC Model. Preprints, *16th AMS Conference on Weather Analysis and Forecasting*, 11–16 January 1998, 1123–1125.

Reed, R. J.; and Hardy, K. R. 1972: A Case Study of Persistent, Intense Clear-Air Turbulence in an Upper-Level Frontal Zone. *J. Appl. Meteor.*, **11**, 541–549.

Reiter, E. R.; and Nania, A. 1964: Jet-Stream Structure and Clear-Air Turbulence. *J. Appl. Meteor.*, **3**, 247–260.

Roach, W. T. 1970: On the Influence of Synoptic Development on the Influence of High Level Turbulence. *Quart. J. Roy. Meteor. Soc.*, **96**, 413–429.

Sharman, R.; Wiener, G.; and Brown, B. 2000: Description and Integration of the NCAR Integrated Turbulence Forecasting Algorithm (ITFA). AIAA 00-0493.

Uccellini, L. W.; Brill, K. F.; Petersen, R. A.; Keyser, D.; Aune, R.; Kocin, P. J.; and des Jardins, M. 1986: A Report on the Upper-Level Wind Conditions Preceding and During the Shuttle Challenger (STS 51L) Explosion. *Bull. Amer. Meteor. Soc.*, **67**, 1248–1265.

Table 1. 44 Case Study NTSB Data Base Summary

NTSB number	Date	Location	Time	HT (MSL)	Type	Case
BFO90LA043	05/11/90	Washington, DC	1700Z	2800 m	CAT	1
MIA90LA152	07/14/90	Miami, FL	1949Z	4100 m	TRW	2
MIA90LA155	07/18/90	Fort Myers, FL	2048Z	10100 m	CAT	3
FTW90LA156	08/09/90	Corpus Christie, TX	1315Z	11000 m	CAT	4
CHI91LA115	03/23/91	Buffalo, NY	2315Z	10300 m	CAT	5
ATL91LA091	05/04/91	Tulsa, OK	2240Z	14300 m	TRW	6
SEA91LA126	06/05/91	Elko, NV	0100Z	Cruise	CAT	7
BFO91LA055	06/16/91	Philadelphia, PA	1900Z	6700 m	TRW	8
NYO91LA164	07/01/91	Newark, NJ	0047Z	11700 m	TRW	9
ATL91LA123	07/04/91	Alma, GA	1607Z	12300 m	TRW	10
FTW92LA001	10/05/91	Little Rock, AR	0730Z	11700 m	TRW	11
FTW92LA142	05/14/92	Palacios, TX	0150Z	4300 m	CLD	12
CHI92LA206	07/02/92	Janesville, WI	0550Z	8700 m	TRW	13
FTW92LA200	08/03/92	Springfield, MO	1915Z	6500 m	TRW	14
BFO93LA048	03/05/93	Philadelphia, PA	2140Z	Finala	CLD	15
MIA93LA090	03/23/93	Jacksonville, FL	2352Z	770 m	TRW	16
DCA93MA033	03/31/93	Anchorage, AK	2034Z	670 m	MTN	17
CHI93LA192	06/04/93	Chicago, IL	2340Z	Climb	CAT	18
CHI93LA224	06/24/93	Baraboo, WI	1729Z	9700 m	CLD	19
MIA93LA151	07/16/93	Caribbean (N of Venezuela)	0815Z	11700 m	CLD	20
ATL93LA159	09/15/93	Atlanta, GA	0145Z	4500 m	TRW	21
MIA94LA010	10/22/93	Atlantic (450NM SE of Miami, FL)	0730Z	11700 m	CAT	22
LAX94LA041	02/12/94	Pacific (10S 157E)	1345Z	11700 m	TRW	23
NYC94LA111	06/29/94	East Hampton, NY	1745Z	8000 m	TRW	24
MIA94LA173	07/05/94	Valdosta, GA	1210Z	6000 m	CAT	25
FTW94LA229	07/07/94	South Bend, IN	2159Z	6700 m	CLD	26
MIA94LA214	09/19/94	West Palm, FL	2239Z	Descent	CLD	27
MIA95LA055	01/06/95	Monroe, LA	1520Z	3062 m	CAT	28
ATL95LA062	03/16/95	Alma, GA	1935Z	12300 m	CAT	29
FTW95LA176	04/19/95	Utopia, TX	0341Z	8300 m	CAT	30
CHI95LA188	06/20/95	Champagne, IL	2310Z	13000 m	TRW	31
CHI95LA271	08/04/95	Grand Rapids, MI	0248Z	9000 m	TRW	32
LAX96LA019	10/17/95	Pacific (40N 152E)	0944Z	11000 m	CAT	33
MIA96LA019	11/07/95	Pensacola, FL	2056Z	6000 m	CAT	34
SEA96LA026	11/25/95	Portland, OR	2323Z	6700 m	CAT	35
LAX96LA090	12/30/95	Honolulu, HI	1943Z	2300 m	TRW	36
MIA96FA064	01/17/96	Cat Island, BA	1938Z	11700 m	TRW	37
FTW96LA107	01/28/96	Bernal, NM (AGL)	2200Z	333 m	MTN	38
FTW96LA157	03/23/96	Taos, NM	1620Z	11000 m	CAT	39
IAD96LA220	04/07/96	300NM SW of Bermuda	0000Z	10300 m	CAT	40
FTW96LA271	06/22/96	Granite, CO	2145Z	8000 m	CAT	41
MIA96LA220	08/29/96	Chattanooga, TN	1953Z	11700 m	CAT	42
LAX97LA051	11/19/96	Bishop, CA	0150Z	9700 m	CAT	43
FTW97LA070	12/20/96	Denver, CO	0050Z	4700 m	MTN	44

Table 2. 44 Case Study Turbulence Categories

Type	Preliminary total	No. of cases lost to type TRW*	Final total
CAT	19	–3	16
TRW	16	–8	8
CLD	6	–2	4
MTN	3	–0	3
TRW*	0		13

Table 3. 44 Case Study Location Distribution

Case location	No. of cases
Warm Ocean	7
Northwest U.S.	5
Southwest U.S.	3
North Central U.S.	6
South Central U.S.	7
Northeast U.S.	6
Southeast U.S.	10

Table 4. 44 Case Study Monthly Distribution

Month	No. of cases	Month	No. of cases	Month	No. of cases	Season	No. of cases
January	3	May	3	September	2	Winter	6
February	1	June	7	October	3	Spring	11
March	6	July	8	November	3	Summer	19
April	2	August	4	December	2	Autumn	8

Table 5. 44 Case Study Diurnal Distribution

Time of day	No. of cases
01–04Z	8
05–08Z	4
09–12Z	2
13–16Z	5
17–20Z	10
21–00Z	15

Table 6. 44 Case Study Altitude Distribution

Altitude	No. of cases
1–3000 m	5
3001–6000 m	5
6001–9000 m	10
9001–12000 m	16
12001–15000 m	4
>15000 m	0

Table 7. Horizontal Cross Sectional Fields Calculated at the Level, Below the Level, and Above the Level of the Accident

Specific Meteorological Fields Used To Derive Predictors
1. Temperature
2. Height
3. Total winds
4. Geostrophic winds
5. Ageostrophic winds
6. Omega
7. Absolute vorticity
8. Relative vorticity
9. Velocity divergence
10. Vertical total wind shear
11. Isentropic potential vorticity
12. Equivalent potential vorticity
13. Potential temperature
14. Equivalent potential temperature
15. Richardson number
16. Thermal wind
17. Relative humidity
18. Lapse rate

Table 8. Vertical Cross Sectional Fields of the Atmosphere From the Surface to 100 mb (~16 km) and Centered on the Accident Location

1. Jet normal and tangential total winds
2. Jet normal and tangential potential temperature
3. Jet normal and tangential equivalent potential temperature
4. Origination-destination total winds
5. Origination-destination potential temperature
6. Origination-destination equivalent potential temperature
7. Origination-destination isentropic potential vorticity
8. Origination-destination equivalent potential vorticity
9. Origination-destination Richardson number
10. Origination-destination relative vorticity
11. Origination-destination relative humidity
12. Origination-destination total vertical wind shear

Vertical Soundings at the Accident Location

1. Skew-t/log-p
2. Richardson number
3. Brunt-vaisala frequency
4. Vertical total wind shear

Table 9. Predictor Fields

1. Immediate upstream curvature
2. Entrance/exit region of the jet stream
3. Sign of omega
4. Lapse rate ≥ moist adiabatic
5. Direction of the ageostrophic wind vector
6. Sign of the horizontal temperature advection
7. Sign of the horizontal advection of the total wind velocity shear
8. Vertical variation of the brunt-vaisala frequency > threshold value
9. Flight level absolute vorticity ≤ 10^{-4} s^{-1}
10. Absolute vorticity averaged over two levels ≤ 10^{-4} s^{-1}
11. Flight level relative vorticity ≤ 0 s^{-1}
12. Relative magnitude of isobaric pv terms
13. Vertical total wind shear > threshold value
14. Relative humidity ≥ 50%
15. Sign of horizontal advection of the vertical lapse rate
16. Ageostrophic wind velocity ≥ threshold value
17. Vertical variation of the Richardson number ≥ threshold value
18. Vertical variation of the total wind velocity shear ≥ threshold value
19. Richardson number ≤ threshold value
20. Convective clouds (all bases) < 100 km from accident location
21. Convective clouds (all bases) < 30 km from accident location
22. Ellrod index values (Ellrod and Knapp 1992)
23. NCSU modification of the Ellrod index (Ellrod index/ipv)

Table 10. Best Predictors for 44 Accident Case Studies (% of 44)

1. Immediate upstream curvature	(98%)
2. Convective clouds (all bases) < 100 km away	(86%)
3. Upward vertical motion	(82%)
4. Layer-averaged absolute vorticity ≤ 10^{-4} s^{-1}	(80%)
5. Jet entrance region	(77%)
6. Higher vertical shear advection	(77%)
7. Lapse rate ≥ moist adiabatic	(77%)
8. Absolute vorticity at flight level ≤ 10^{-4} s^{-1}	(75%)
9. Convective clouds (all bases) < 30 km away	(74%)
10. Horizontal cold advection	(73%)
11. Flight level relative vorticity ≤ 0 s^{-1}	(68%)
12. Leftward-directed $v_{ageostrophic}$ flow	(64%)

Table 11. Best Predictors for CAT Accident Case Studies (% of 16)

1. Immediate upstream curvature	(100%)
2. Jet entrance region	(81%)
3. Upward vertical motion	(81%)
4. Convective clouds (all bases) < 100 km away	(75%)
5. Lapse rate ≥ moist adiabatic	(75%)
6. Leftward-directed $v_{ageostrophic}$ flow	(75%)
7. Layer-averaged absolute vorticity ≤ 10^{-4} s^{-1}	(69%)
8. Horizontal cold advection	(69%)
9. Higher vertical shear advection	(69%)
10. Flight level absolute vorticity ≤ 10^{-4} s^{-1}	(63%)
11. Convective clouds (all bases) < 30 km away	(63%)
12. Flight level relative vorticity < 0 s^{-1}	(56%)

Table 12. Best Predictors for TRW* Accident Case Studies (% of 13)

1. Flight level absolute vorticity ≤ 10^{-4} s^{-1}	(100%)
2. Layer-averaged absolute vorticity ≤ 10^{-4} s^{-1}	(100%)
3. Convective clouds (all bases) ≤ 100 km away	(93%)
4. Immediate upstream curvature	(92%)
5. Lapse rate ≥ moist adiabatic	(85%)
6. Convective clouds (all bases) ≤ 30 km away	(83%)
7. Upward vertical motion	(77%)
8. Flight level relative vorticity ≤ 0 s^{-1}	(77%)
9. Higher vertical shear advection	(77%)
10. Jet entrance region	(69%)
11. Cold lapse rate advection	(69%)
12. Horizontal cold advection	(62%)

Table 13. Best Predictors for TRW Accident Case Studies (% of 8)

1. Convective clouds (all bases) ≤ 100 km away	(100%)
2. Immediate upstream curvature	(100%)
3. Horizontal cold advection	(100%)
4. Convective clouds (all bases) ≤ 30 km away	(88%)
5. Upward vertical motion	(88%)
6. Higher vertical shear advection	(88%)
7. Flight level absolute vorticity ≤ 10^{-4} s^{-1}	(75%)
8. Layer-averaged absolute vorticity ≤ 10^{-4} s^{-1}	(75%)
9. Relative vorticity ≤ 0 s^{-1}	(75%)
10. Cold lapse rate advection	(75%)
11. Relative humidity ≥ 50%	(64%)
12. Jet entrance region	(64%)

Table 14. Best Predictors for CLD Accident Case Studies (% of 4)

1. Immediate upstream curvature	(100%)
2. Jet entrance region	(100%)
3. Convective clouds (all bases) ≤ 100 km away	(100%)
4. Upward vertical motion	(100%)
5. Cold lapse rate advection	(100%)
6. Higher vertical shear advection	(100%)
7. Convective clouds (all bases) ≤ 30 km away	(75%)
8. Flight level absolute vorticity ≤ 10^{-4} s^{-1}	(75%)
9. Layer-averaged absolute vorticity ≤ 10^{-4} s^{-1}	(75%)
10. Relative vorticity ≤ 0 s^{-1}	(75%)
11. Horizontal cold advection	(75%)
12. Relative humidity ≥ 50%	(75%)

Table 15. Best Predictors for MTN Accident Case Studies (% of 3)

1. Vertical shear ≥ threshold value	(100%)
2. Immediate upstream curvature	(100%)
3. Flight level absolute vorticity ≤ 10^{-4} s^{-1}	(100%)
4. Convective clouds (all bases) ≤ 100 km away	(67%)
5. Convective clouds (all bases) ≤ 30 km away	(67%)
6. Upward vertical motion	(67%)
7. Horizontal cold advection	(67%)
8. Cold lapse rate advection	(67%)
9. Lapse rate ≥ moist adiabatic	(67%)
10. Layer-averaged absolute vorticity ≤ 10^{-4} s^{-1}	(67%)
11. Higher vertical shear advection	(67%)
12. Vertical variation of the Richardson number > threshold value	(67%)

NTSB Identification: **FTW94LA229**. The docket is stored in the (offline) NTSB Imaging System.

Scheduled 14 CFR 121 operation of SOUTHWEST AIRLINES, CO. (D.B.A. SOUTHWEST AIRLINES)
Accident occurred JUL-07-94 at SOUTH BEND, IN
Aircraft: BOEING 737-2H4, registration: N668SW
Injuries: 1 Serious, 104 Uninjured.

A FLIGHT ATTENDANT WORKING IN THE AFT GALLEY FELL TO THE FLOOR SERIOUSLY INJURING HER BACK WHEN THE AIRCRAFT ENCOUNTERED TURBULENCE. ACCORDING TO THE FLIGHT CREW, RADAR WAS USED TO AVOID WEATHER AS THE AIRCRAFT APPROACHED SOUTH BEND, INDIANA. THERE HAD BEEN NO PILOT REPORTS OF TURBULENCE, AND THE COMPANY DISPATCHER WEATHER PACKAGE DID NOT REPORT TURBULENCE. AS THE FLIGHT CLIMBED THROUGH FL206, MODERATE TURBULENCE WAS ENCOUNTERED FOR SEVERAL SECONDS. THE AIRCRAFT THEN ENTERED VISUAL METEOROLOGICAL CONDITIONS AND SMOOTH AIR. THE CAPTAIN STATED THAT THE UNEXPECTED TURBULENCE STARTED AND STOPPED SO QUICKLY THAT HE DID NOT HAVE TIME TO WARN THE FLIGHT ATTENDANTS. THE SEAT BELT SIGN WAS ILLUMINATED AT THE TIME THE TURBULENCE WAS ENCOUNTERED.

Probable Cause

THE ENCOUNTER WITH UNFORCASTED AND UNREPORTED TURBULENCE.

(a) 7 July 1994 NTSB accident narrative.

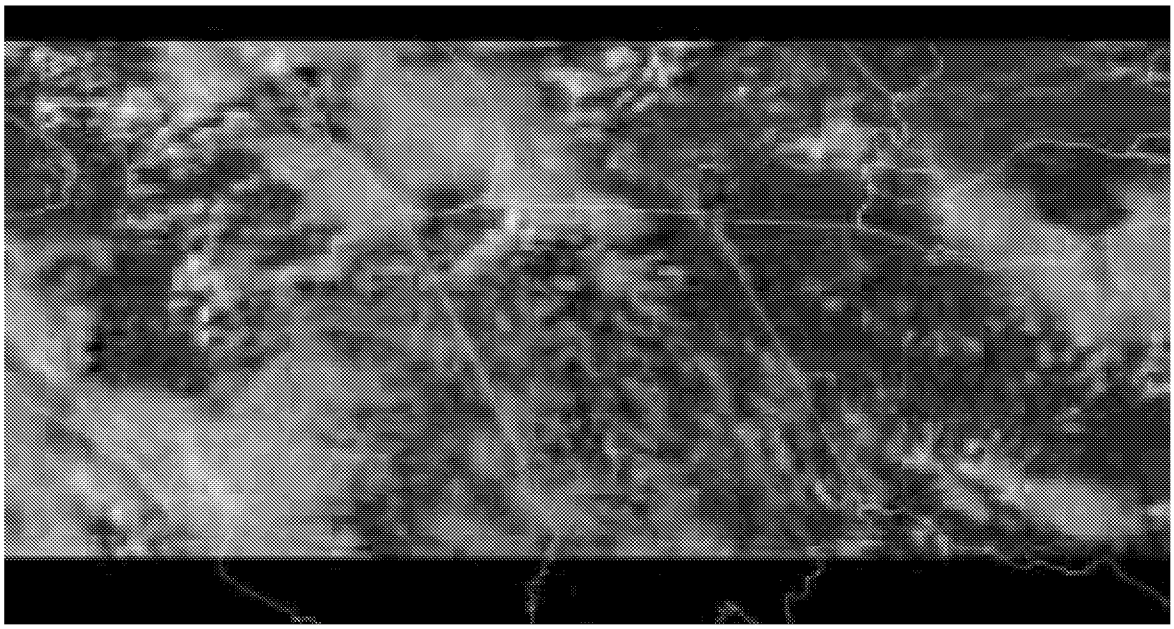

(b) GOES visible satellite imagery at accident location of South Bend, IN, valid at 2201 UTC 7 July 1994.

Figure 1. South Bend, IN, case study.

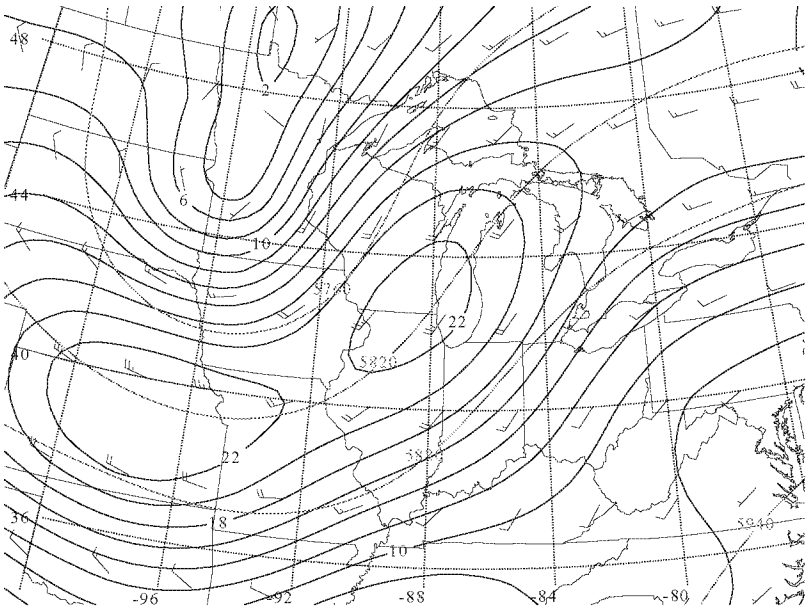

(a) Height (light solid in m), wind barbs (half barb = 5 ms^{-1}; full barb = 10 ms^{-1}; triangle = 50 ms^{-1}), and isotachs (dark solid in ms^{-1}).

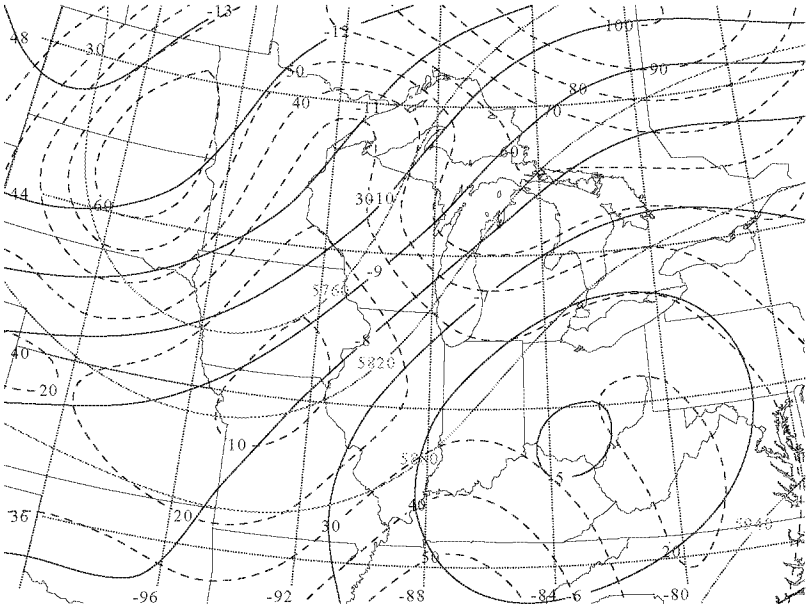

(b) Height (light solid in m), temperature (dark solid in C), and relative humidity (dashed in %).

Figure 2. 0000 UTC 8 July 1994 NCEP Reanalyses 500 mb.

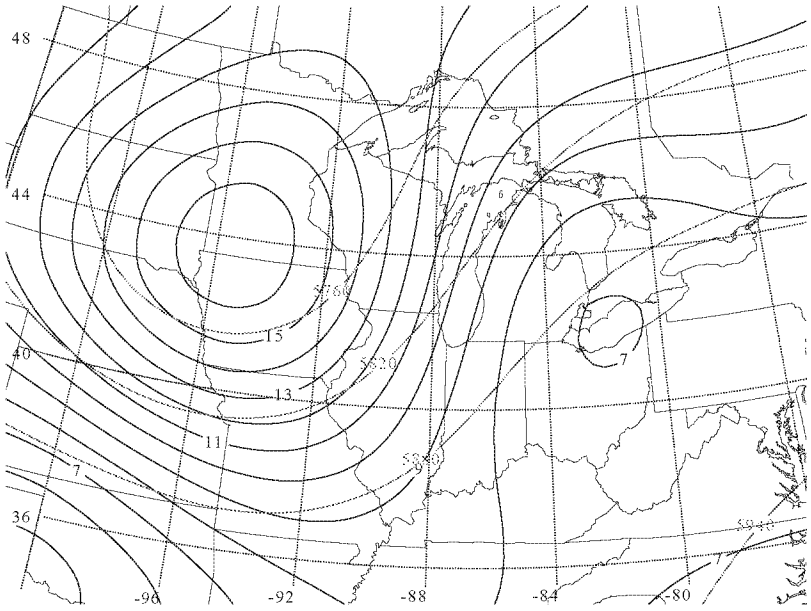

(c) Height (light solid in m) and absolute vorticity (dark solid in $s^{-1} \times 10^{-5}$).

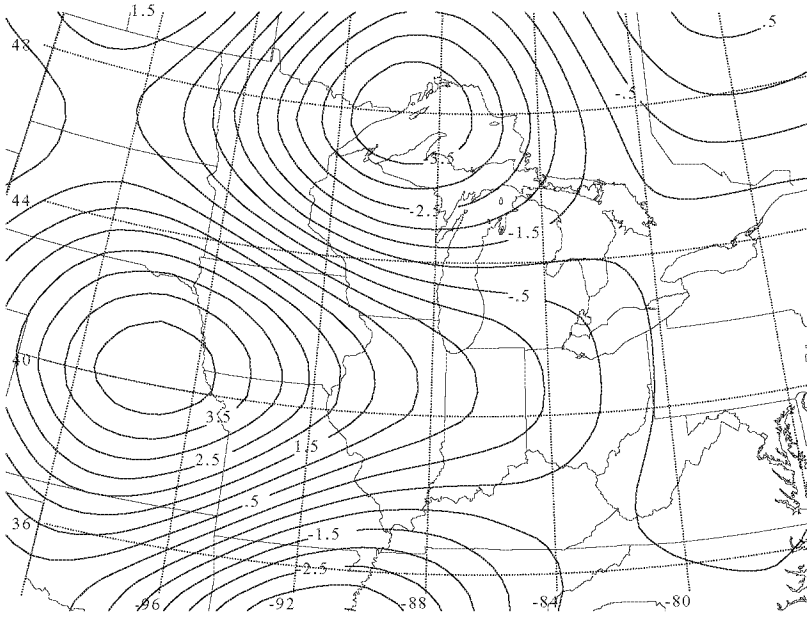

(d) Omega (solid in microbar/s).

Figure 2. Continued.

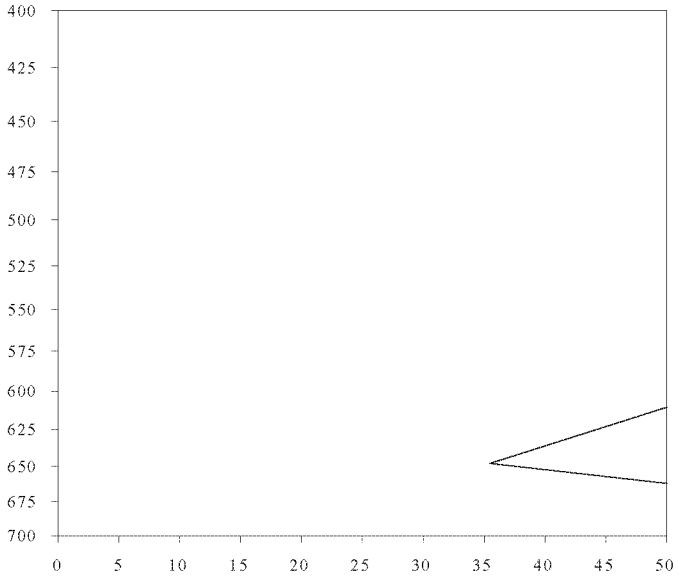

(e) Vertical profile of Richardson number.

Figure 2. Concluded.

NTSB Identification: **ATL95LA062**. The docket is stored in the (offline) NTSB Imaging System.

Scheduled 14 CFR 121 operation of DELTA AIR LINES
Accident occurred MAR-16-95 at ALMA, GA
Aircraft: BOEING 727-200, registration: N295WA
Injuries: 1 Serious, 5 Minor, 132 Uninjured.

WHILE EN ROUTE FROM NASSAU, BAHAMAS TO ATLANTA, GEORGIA THE DOMESTIC PASSENGER FLIGHT, A BOEING 727-200, ENCOUNTERED CLEAR AIR TURBULENCE AT FL370. THE AIRCRAFT HAD EXPERIENCE LIGHT CHOP PRIOR TO REACHING FL370, AND THE FASTEN SEAT BELT SIGN WAS ILLUMINATED. VISUAL METEOROLOGICAL CONDITIONS EXISTED AT FL370, AND THE CREW HAD NO INDICATION THAT THEY MAY ENCOUNTER ANY SEVERE TURBULENCE. BETWEEN 1435:31.42 AND 1435:31.45, WITHOUT WARNING, THE AIRCRAFT ROLLED 52.2 DEGREES RIGHT AND 58.9 DEGREES LEFT. THE VERTICAL ACCELERATION REACHED A MAXIMUM OF 1.93 "G" AND A MINIMUM OF -0.80 "G" WITHIN THE SAME TIME INTERVAL. THE AIRCRAFT LOST 1,500 FEET IN ALTITUDE.
Probable Cause
THE AIRCRAFT'S ENCOUNTER WITH UNFORECAST CLEAR AIR TURBULENCE.

(a) 16 March 1995 NTSB accident narrative.

(b) GOES visible satellite imagery at accident location of Alma, GA, valid at 1932 UTC 16 March 1995.

Figure 3. Alma, GA, case study.

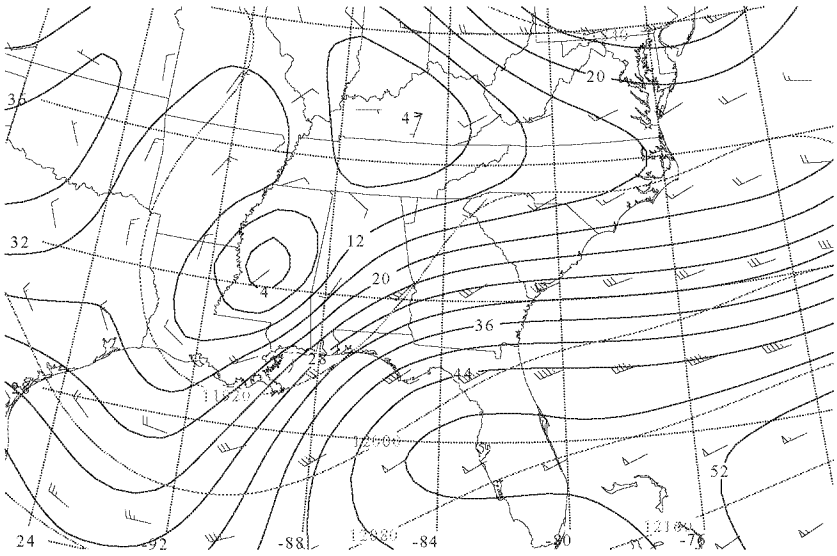

(a) Height (light solid in m), wind barbs (half barb = 5 ms^{-1}; full barb = 10 ms^{-1}; triangle = 50 ms^{-1}), and isotachs (dark solid in ms^{-1}).

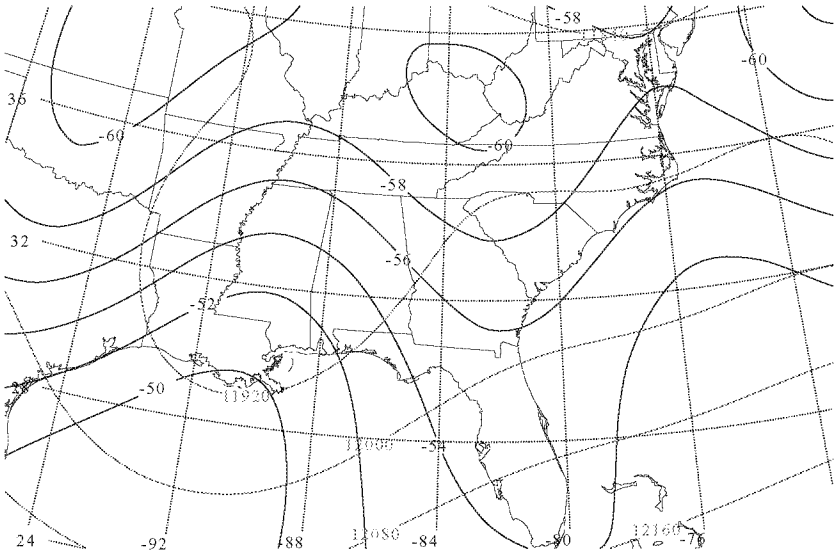

(b) Height (light solid in m) and temperature (dark solid in C).

Figure 4. 1800 UTC 16 March 1995 NCEP Reanalyses 200 mb.

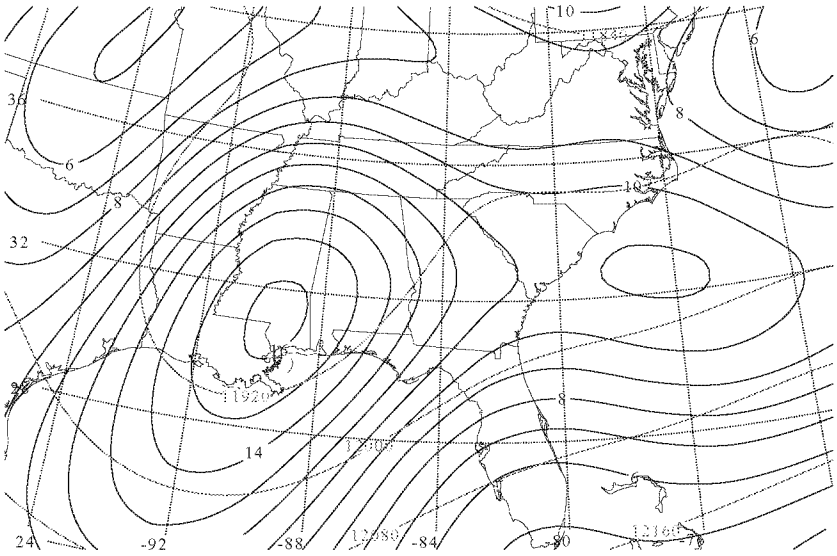

(c) Height (light solid in m) and absolute vorticity (dark solid in $s^{-1} \times 10^{-5}$).

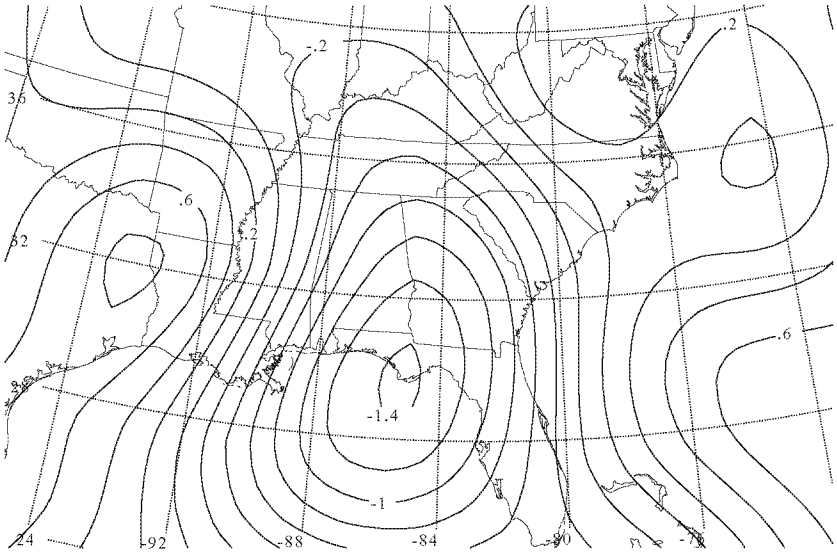

(d) Omega (solid in microbar/s).

Figure 4. Continued.

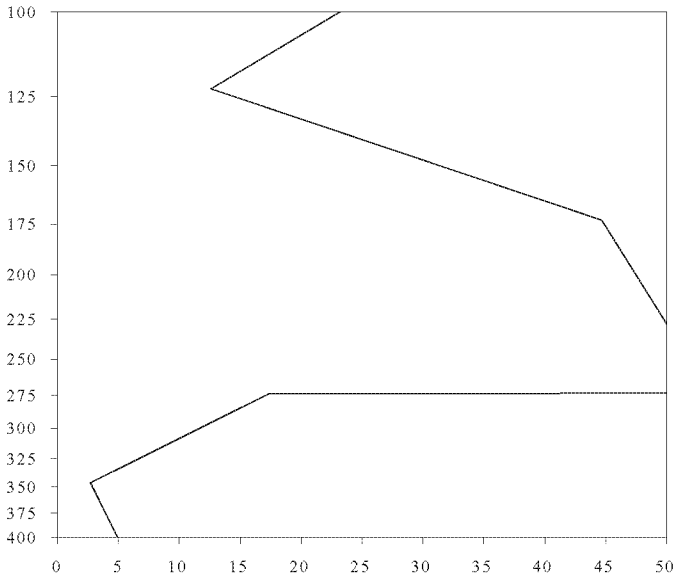

(e) Vertical profile of Richardson number.

Figure 4. Concluded.

NTSB Identification: **FTW96LA271**. The docket is stored in the (offline) NTSB Imaging System.

Scheduled 14 CFR 121 operation of FRONTIER AIRLINES
Accident occurred JUN-22-96 at GRANITE, CO
Aircraft: Boeing 737-201, registration: N207AU
Injuries: 1 Serious, 2 Minor, 95 Uninjured.

The crew had been forewarned to expect severe turbulence on descent into the Denver area. The "Fasten Seat Belts" sign was turned on, and flight attendants were instructed to make sure everyone was seated with their seat belts fastened. An elderly woman got up and walked towards the aft lavatory. Light turbulence was encountered as a flight attendant attempted to seat the passenger in a jump seat. Before seat belts could be fastened, the airplane encountered severe turbulence. The passenger and flight attendant were thrown around the cabin, sustaining a serious injury and minor injury, respectively. Another flight attendant and a passenger also sustained minor injuries.
Probable Cause
An encounter with clear air turbulence.

(a) 22 June 1996 NTSB accident narrative.

(b) GOES visible satellite imagery at accident location of Granite, CO, valid at 2145 UTC 22 June 1996.

Figure 5. Granite, CO, case study.

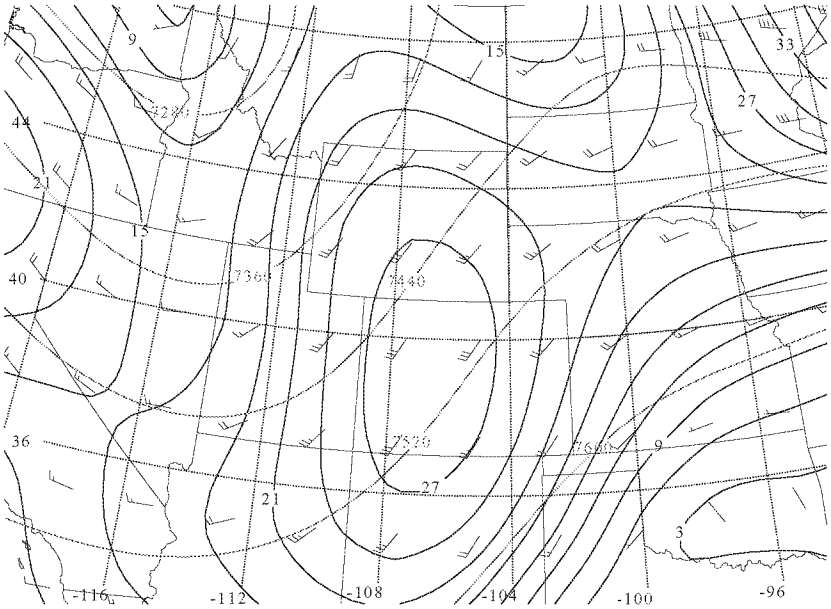

(a) Height (light solid in m), wind barbs (half barb = 5 ms^{-1}; full barb = 10 ms^{-1}; triangle = 50 ms^{-1}), and isotachs (dark solid in ms^{-1}).

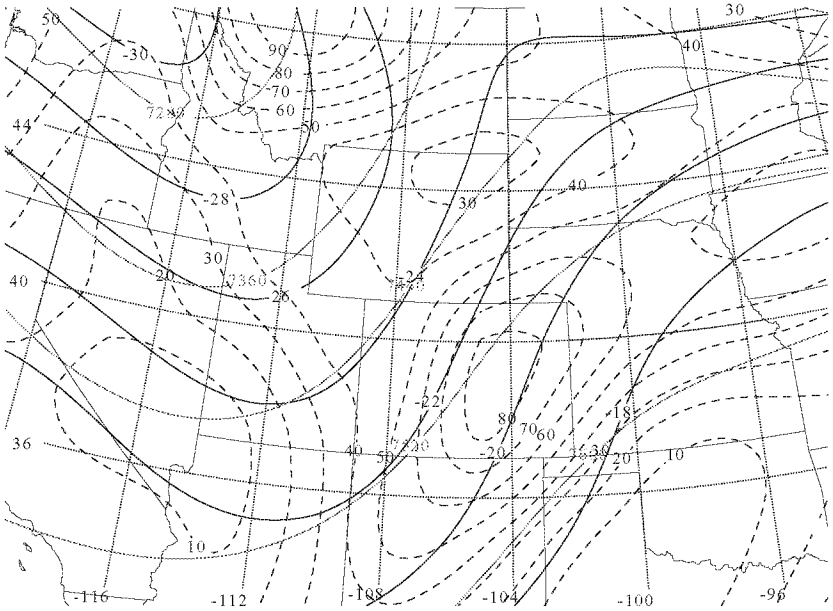

(b) Height (light solid in m), temperature (dark solid in C), and relative humidity (dashed in %).

Figure 6. 1800 UTC 22 June 1996 NCEP Reanalyses 300 mb.

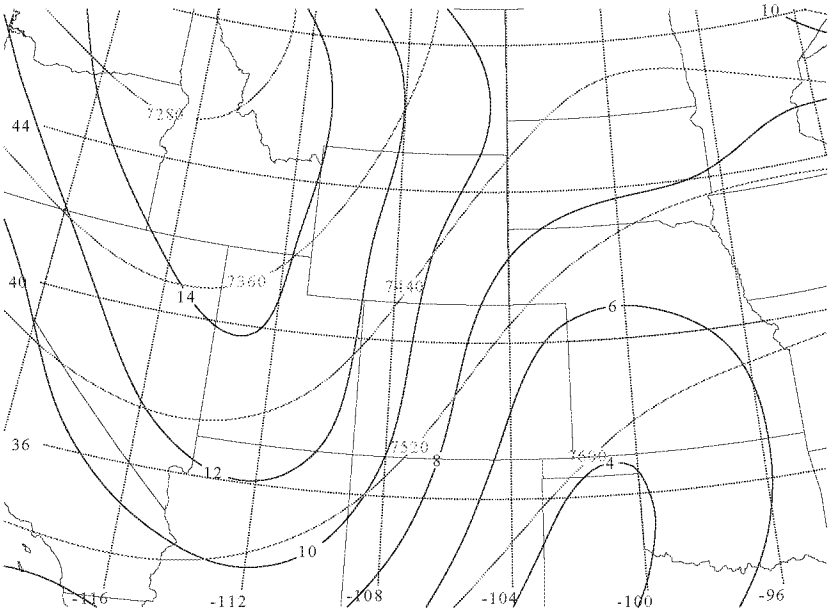

(c) Height (light solid in m) and absolute vorticity (dark solid in $s^{-1} \times 10^{-5}$).

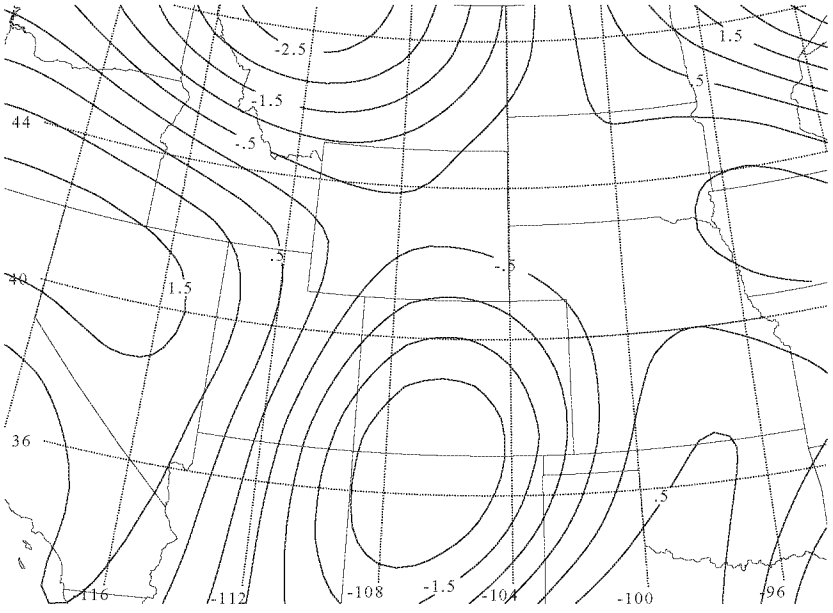

(d) Omega (solid in microbar/s).

Figure 6. Continued.

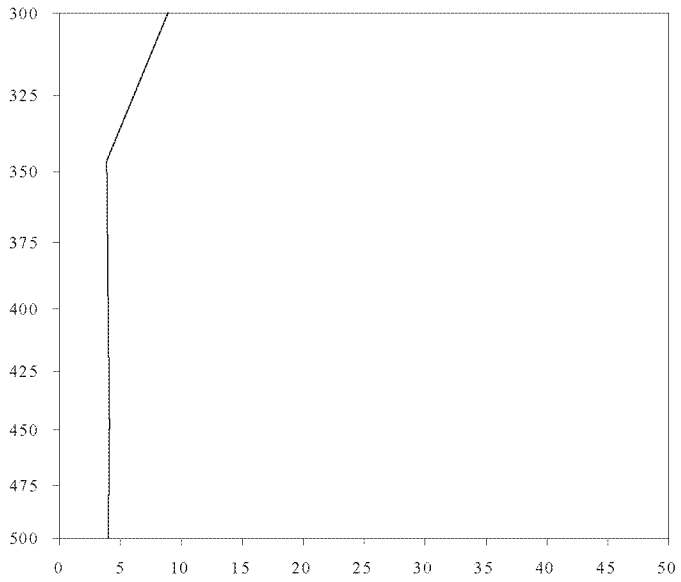

(e) Vertical profile of Richardson number.

Figure 6. Concluded.

NTSB Identification: **MIA90LA152** For details, refer to NTSB microfiche number **43222A**

a

Scheduled 14 CFR 129 operation of BRITISH AIRWAYS
Accident occurred JUL-14-90 at MIAMI, FL
Aircraft: BOEING 747-136, registration: GAWNL
Injuries: 2 Serious, 18 Minor, 363 Uninjured.

FLT ENCOUNTERED SEVERE TURBULENCE WHILE DESCENDING THROUGH 12,300 FEET ON APPROACH TO MIAMI INTERNATIONAL AIRPORT. WEATHER STUDIES INDICATED THE AIRCRAFT WAS IN AT LEAST MODERATE THUNDERSTORM ACTIVITY AND NEAR AN AREA OF VERY HEAVY OR LEVEL 4 ACTIVITY. FLIGHT RECORDER DATA INDICATED PEAK G FORCES WERE ENCOUNTERED 40 SECONDS AFTER TURBULENCE ENCOUNTER. PEAK G FORCES WERE FROM 1.5 TO -0.5 G OVER A THREE SECOND PERIOD.

Probable Cause

THE INADVERTENT ENCOUNTER WITH SEVERE TURBULENCE WHILE OPERATING IN AN AREA OF THUNDERSTORM ACTIVITY.

(a) 14 July 1990 NTSB accident narrative.

(b) GOES visible satellite imagery at accident location of Miami, FL, valid at 2001 UTC 14 July 1990.

Figure 7. Miami, FL, case study.

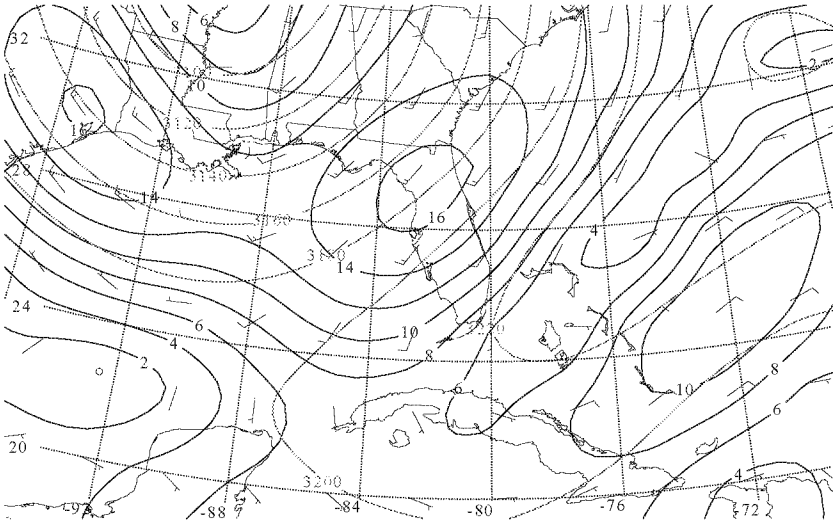

(a) Height (light solid in m), wind barbs (half barb = 5 ms^{-1}; full barb = 10 ms^{-1}; triangle = 50 ms^{-1}), and isotachs (dark solid in ms^{-1}).

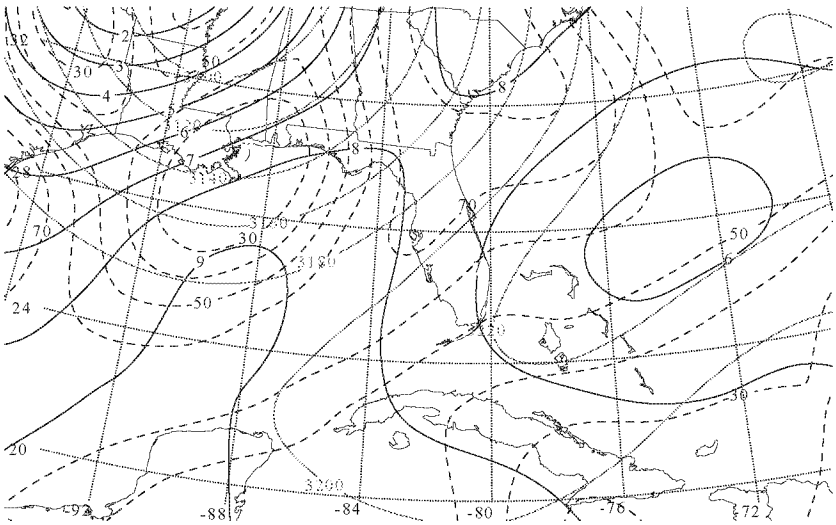

(b) Height (light solid in m), temperature (dark solid in C), and relative humidity (dashed in %).

Figure 8. 1800 UTC 14 July 1990 NCEP Reanalyses 700 mb.

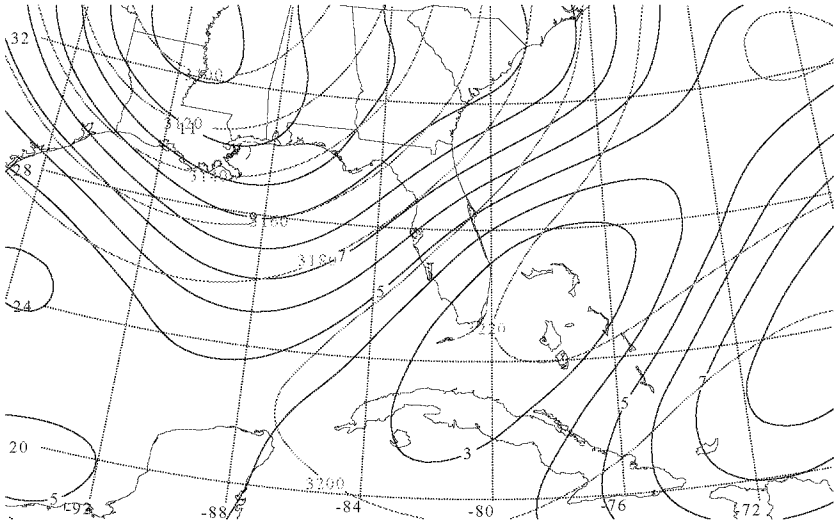

(c) Height (light solid in m) and absolute vorticity (dark solid in $s^{-1} \times 10^{-5}$).

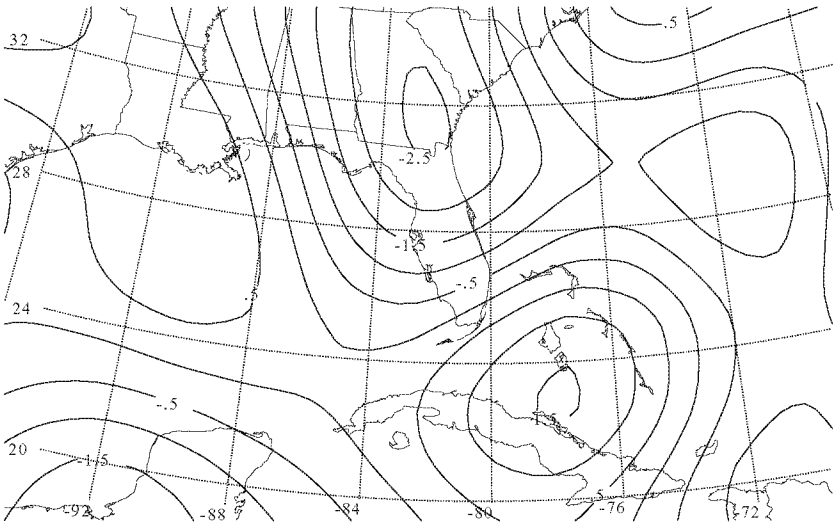

(d) Omega (solid in microbar/s).

Figure 8. Continued.

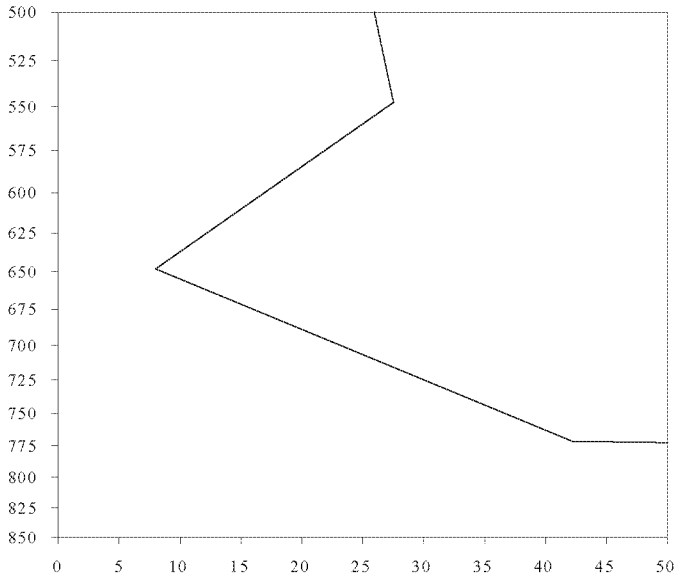

(e) Vertical profile of Richardson number.

Figure 8. Concluded.

NTSB Identification: **MIA90LA155** For details, refer to NTSB microfiche number **41918A**

Scheduled 14 CFR 121 operation of AMERICAN AIRLINES, INC.
Accident occurred JUL-18-90 at FORT MYERS, FL
Aircraft: BOEING 727-223, registration: N6834
Injuries: 1 Serious, 1 Minor, 150 Uninjured

AN AMERICAN AIRLINES, BOEING 727-223, WAS IFR AT FLIGHT LEVEL 30,200. THE AIRPLANE WAS 15 NAUTICAL MILES, NORTHWEST OF FORT MYERS, FLORIDA, IN A DESCENT TO MIAMI INTERNATIONAL AIRPORT, MIAMI, FLORIDA, WHEN IT EXPERIENCED AN UNFORECASTED ENCOUNTER WITH WEATHER (SEVER TURBLENCE). THE AIRPLANE WAS NOT DAMAGED. ONE FLIGHT ATTENDANT SUSTAINED SERIOUS INJURY, AND ONE PASSENGER SUSTAINED MINOR INJURIES. THE AIRPLANE ARRIVED AT DESTINATION AIRPORT WITHOUT FIRTHER INCIDENT. ANALYSIS OF THE FLIGHT DATA RECORDER REVEALED THE AIRPLANE WAS SUBJECTED TO A SERIES OF OSCILLATING VERTICAL ("G") LOADS FOR A PERIOD OF 50 SECONDS. THE MAXIMUM G LOAD WAS 1.94, AND THE MINIMUM WAS -0.55.
Probable Cause
UNFORECASTED ENCOUNTER WITH WEATHER. THE AIRPLANE ENCOUNTERED SEVERE TURBLENCE DURING ENROUTE DESCENT, RESULTING IN ONE FLIGHT ATTENDANT SUSTAINING SERIOUS INJURY, AND ONE PASSENGER SUSTAINING MINOR INJURY.

(a) 18 July 1990 NTSB accident narrative.

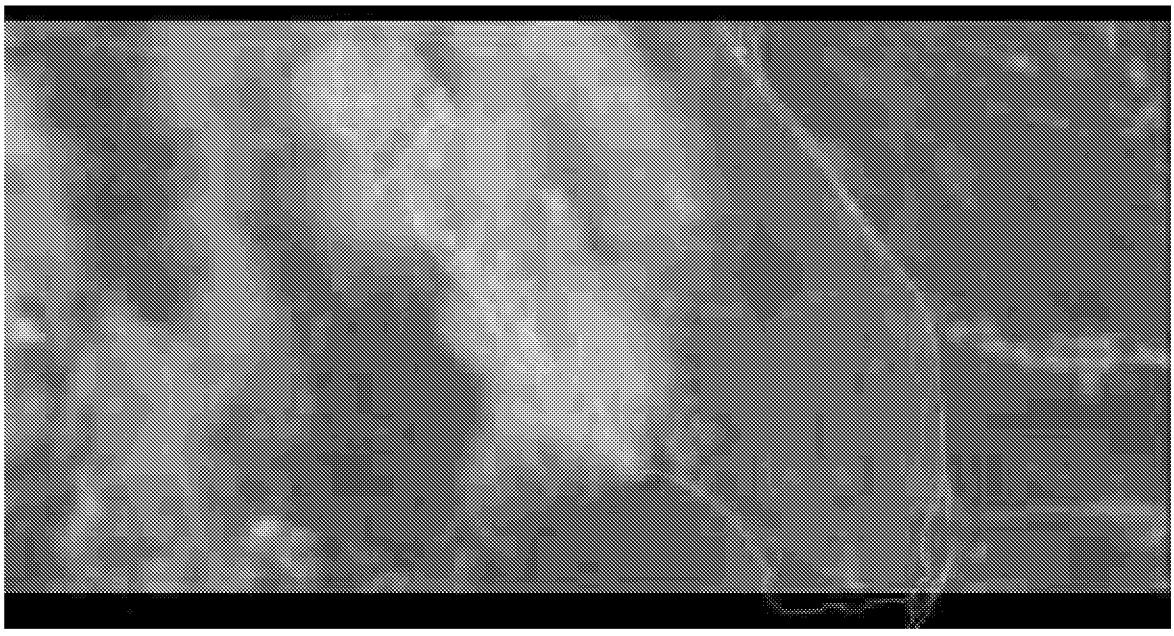

(b) GOES visible satellite imagery at accident location of Fort Myers, FL, valid at 2101 UTC 18 July 1990.

Figure 9. Fort Myers, FL, case study.

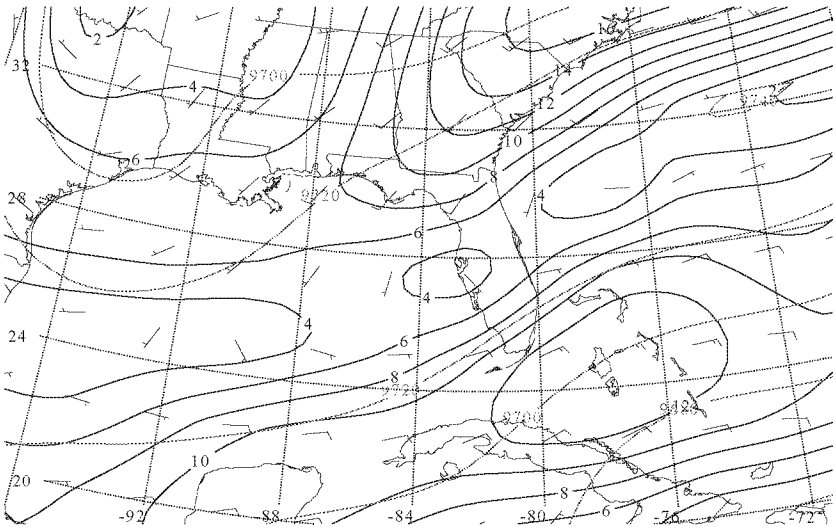

(a) Height (light solid in m), wind barbs (half barb = 5 ms^{-1}; full barb = 10 ms^{-1}; triangle = 50 ms^{-1}), and isotachs (dark solid in ms^{-1}).

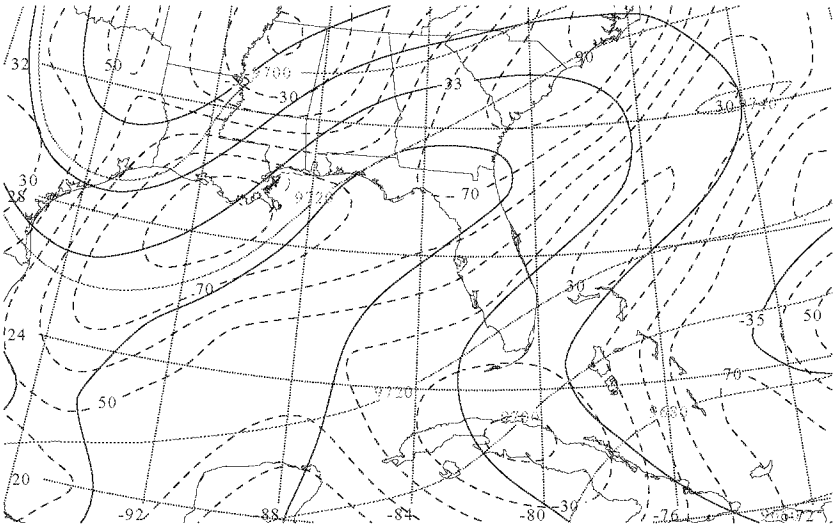

(b) Height (light solid in m), temperature (dark solid in C), and relative humidity (dashed in %).

Figure 10. 1800 UTC 18 July 1990 NCEP Reanalyses 300 mb.

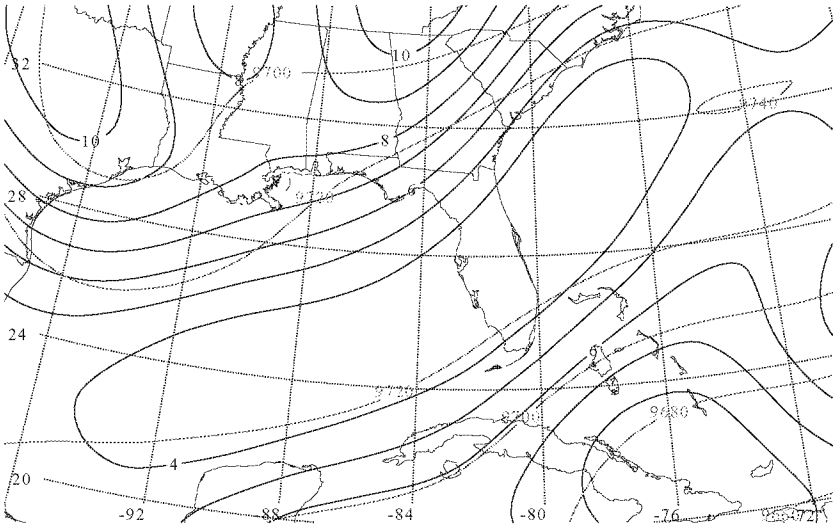

(c) Height (light solid in m) and absolute vorticity (dark solid in $s^{-1} \times 10^{-5}$).

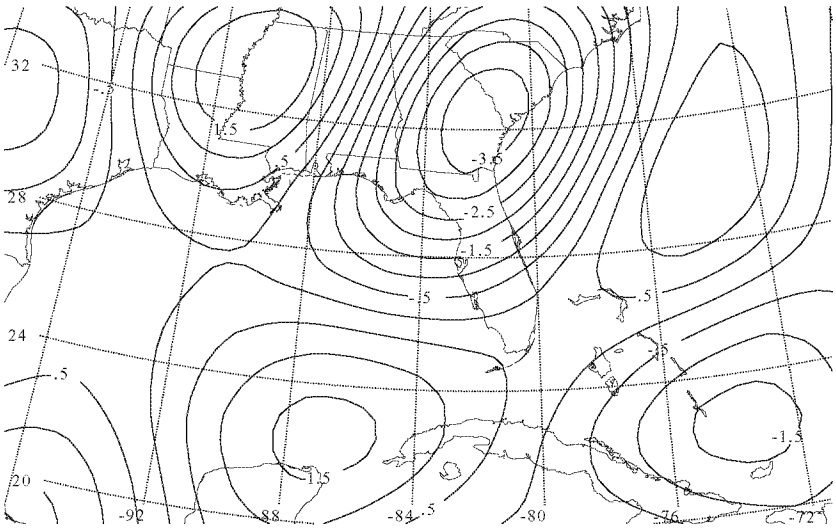

(d) Omega (solid in microbar/s).

Figure 10. Continued.

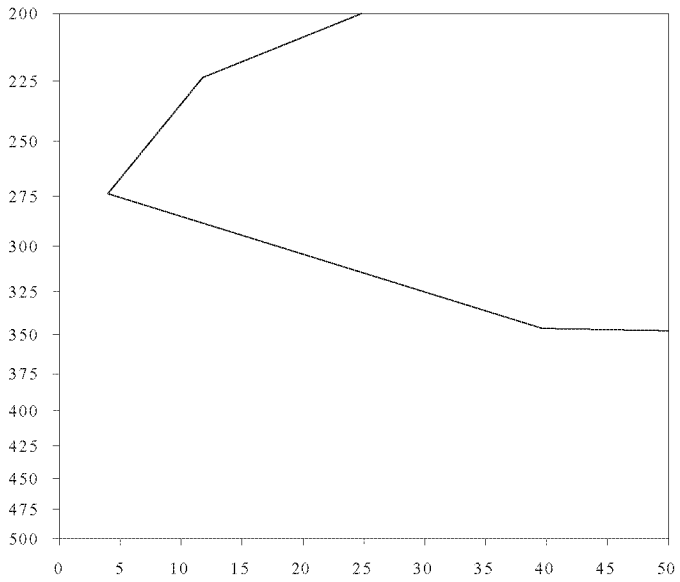

(e) Vertical profile of Richardson number.

Figure 10. Concluded.

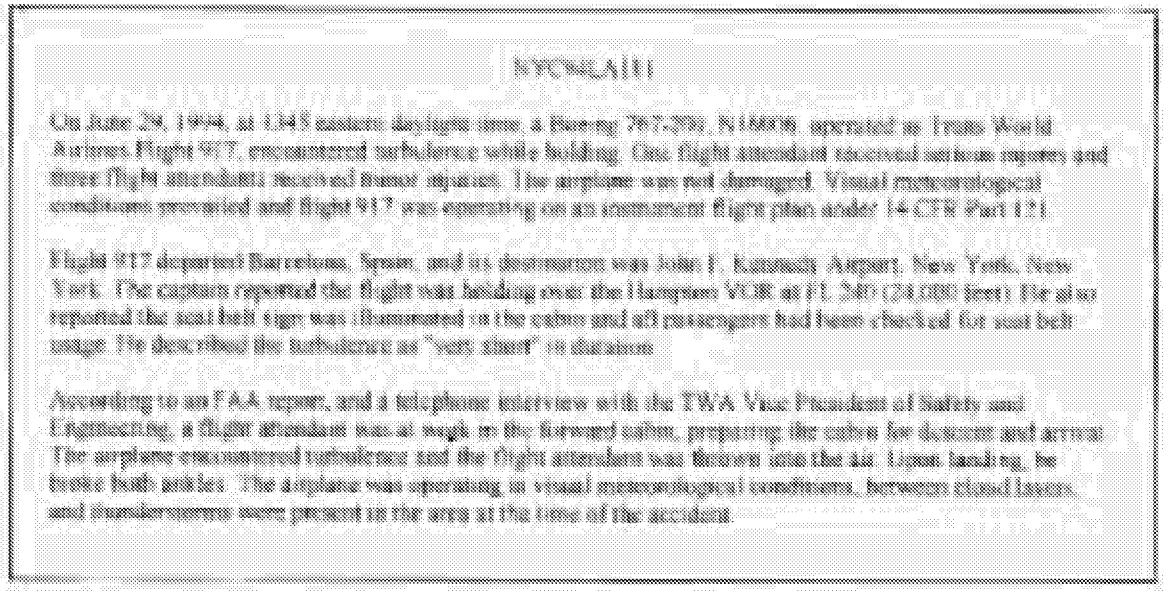

(a) 29 June 1994 NTSB accident narrative.

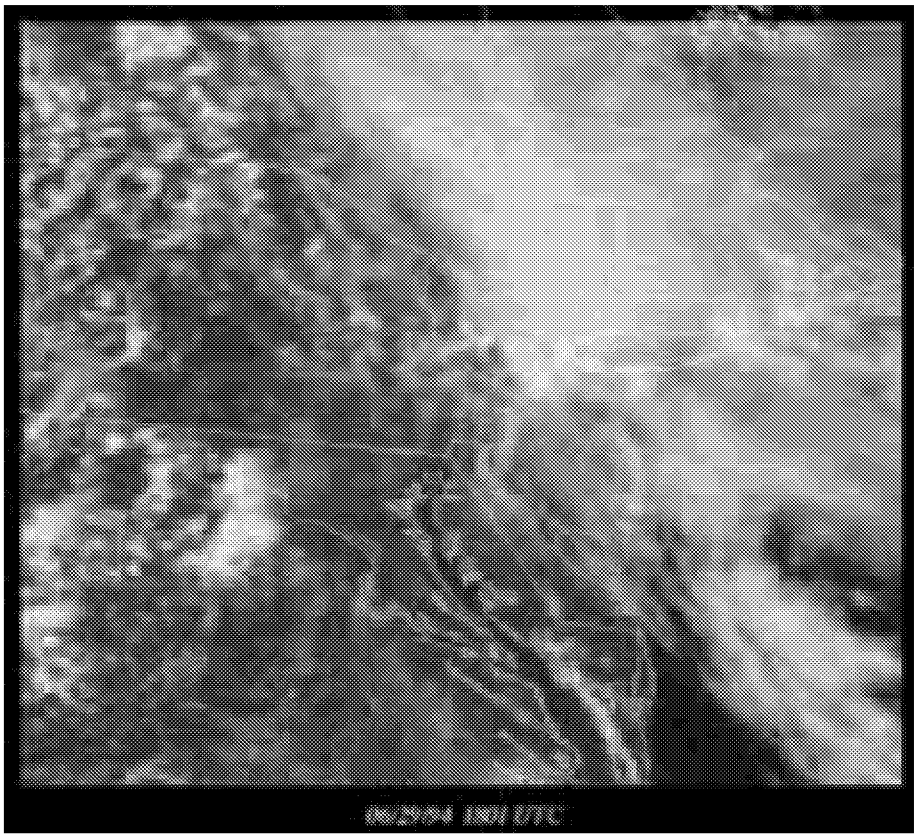

(b) GOES visible satellite imagery at accident location of East Hampton, NY, valid at 1801 UTC 29 June 1994.

Figure 11. East Hampton, NY, case study.

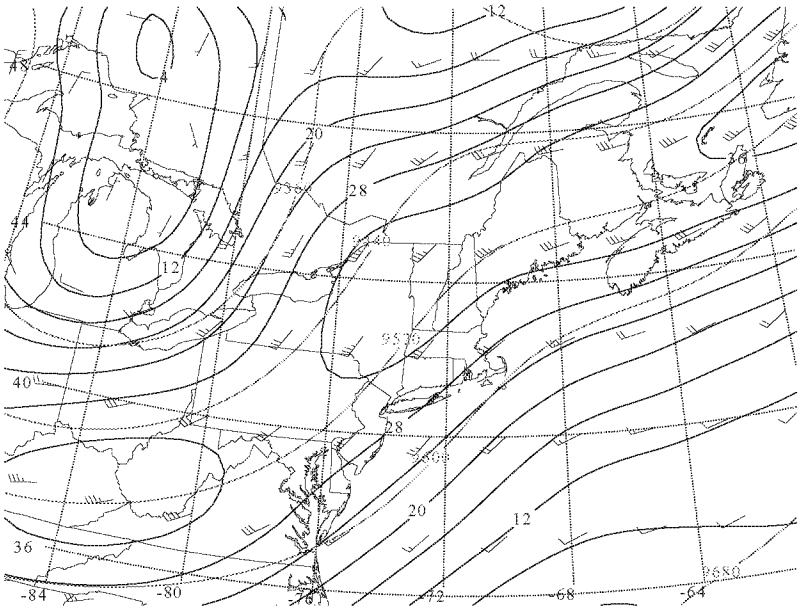

(a) Height (light solid in m), wind barbs (half barb = 5 ms^{-1}; full barb = 10 ms^{-1}; triangle = 50 ms^{-1}), and isotachs (dark solid in ms^{-1}).

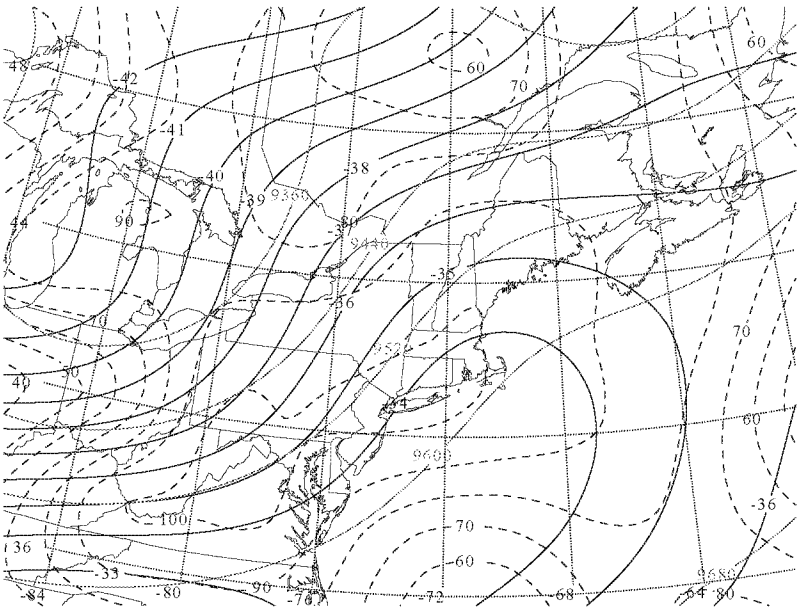

(b) Height (light solid in m), temperature (dark solid in C), and relative humidity (dashed in %).

Figure 12. 1800 UTC 29 June 1994 NCEP Reanalyses 300 mb.

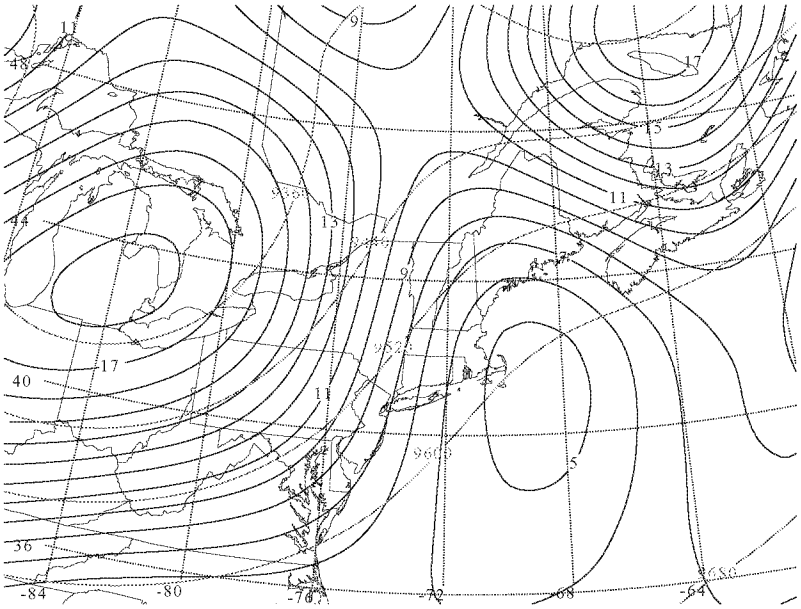

(c) Height (light solid in m) and absolute vorticity (dark solid in $s^{-1} \times 10^{-5}$).

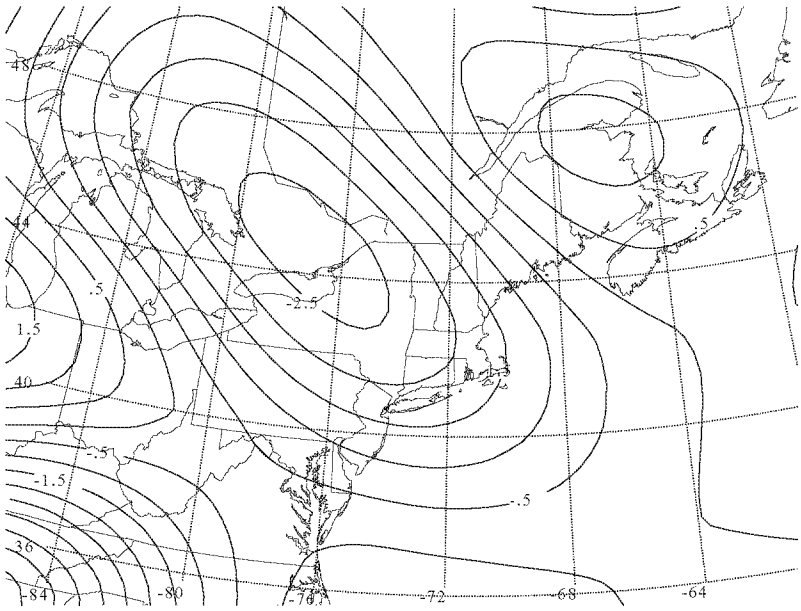

(d) Omega (solid in microbar/s).

Figure 12. Continued.

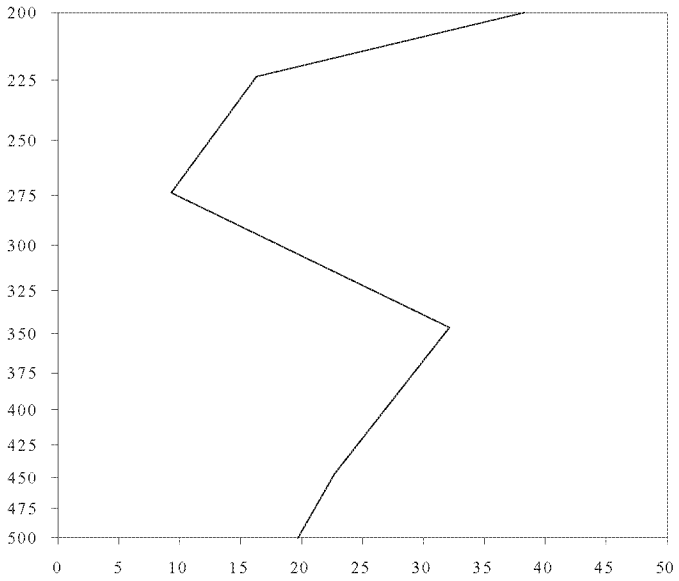

(e) Vertical profile of Richardson number.

Figure 12. Concluded.

CHI95LA271

On August 4, 1995, at 2248 eastern daylight time (edt), a Boeing 757, N509US, operated as Flight 52 by Northwest Airlines, Incorporated, of Minneapolis, Minnesota, and piloted by airline transport rated crew, encountered sudden, moderate, turbulence at flight level 270. The 14 CFR Part 121 flight was operating on an IFR flight plan. One passenger received serious injuries as she was exiting the lavatory when the airplane encountered the turbulence. The seven person flight crew and 120 passengers reported no injuries. The flight departed San Francisco, California, at 1852 edt.

According to the pilot's written statement, the airplane had descended from flight level 410 and had just leveled off at flight level 270, about 25 nautical miles east of Grand Rapids, Michigan, when it encountered the sudden, moderate turbulence. He said the airplane's weather radar was on the 80 mile scan and showed no weather. He said the seat belt sign had been put on and an announcement was made advising the passengers to expect "bumps" on the approach into the Detroit Metropolitan Wayne County Airport, Detroit, Michigan. The company's Director of Flight Safety said the seat belt sign was "...turned on at the top of [the] descent which would have been about 5 minutes... prior to the encounter with the turbulence."

The director said the flight attendants reports concerning the incident did not "...indicate that anyone saw the lady enter the lavatory." He said it is presumed that the passenger was in the lavatory when the seat belt sign was turned on. The airplane's lavatories are equipped with a public address speaker, flight attendant call button, and a sign that reads: "Return To Seat" when the seat belt sign is illuminated in the passenger cabin.

The first officer said the flight was initially cleared to flight level 230. However, according to her statement, the FAA controller changed the clearance to flight level 270 because the flight would have "...the best ride..." at that altitude.

According to the airline's dispatch/meteorology department weather data, the area around Flight 52 had been experiencing 3/10's coverage of level three and four thunderstorms.

(a) 4 August 1995 NTSB accident narrative.

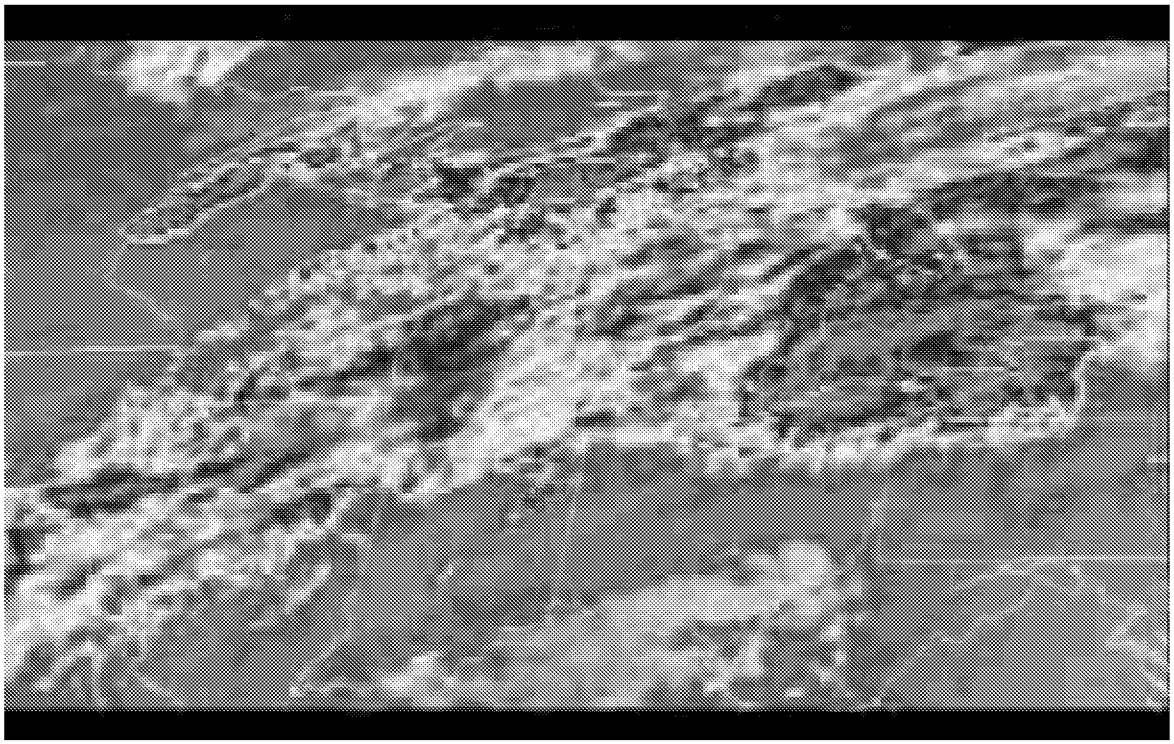

(b) GOES infrared satellite imagery at accident location of Grand Rapids, MI, valid at 0245 UTC 4 August 1995.

Figure 13. Grand Rapids, MI, case study.

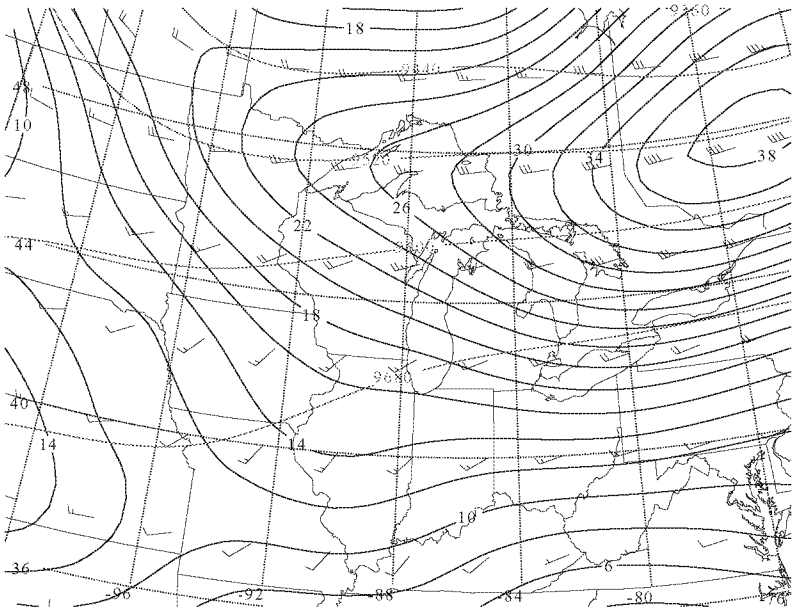

(a) Height (light solid in m), wind barbs (half barb = 5 ms^{-1}; full barb = 10 ms^{-1}; triangle = 50 ms^{-1}), and isotachs (dark solid in ms^{-1}).

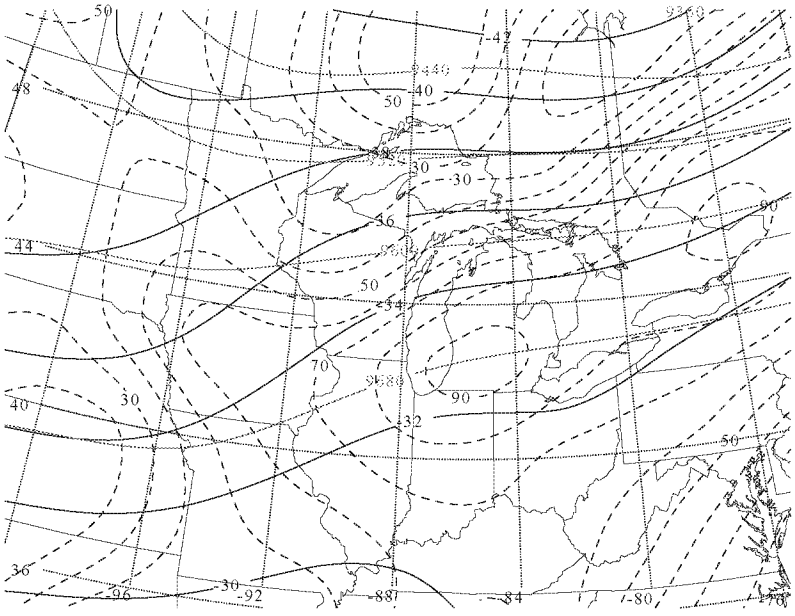

(b) Height (light solid in m), temperature (dark solid in C), and relative humidity (dashed in %).

Figure 14. 0000 UTC 4 August 1995 NCEP Reanalyses 300 mb.

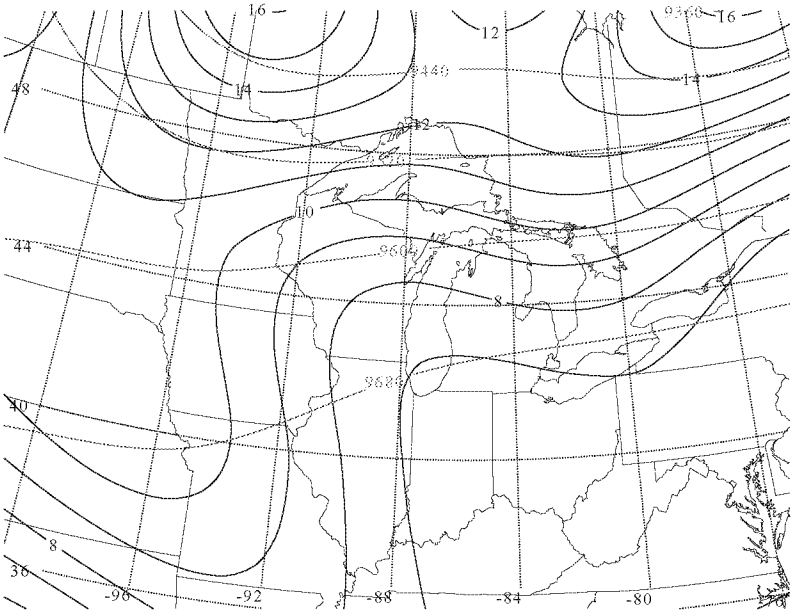

(c) Height (light solid in m) and absolute vorticity (dark solid in $s^{-1} \times 10^{-5}$).

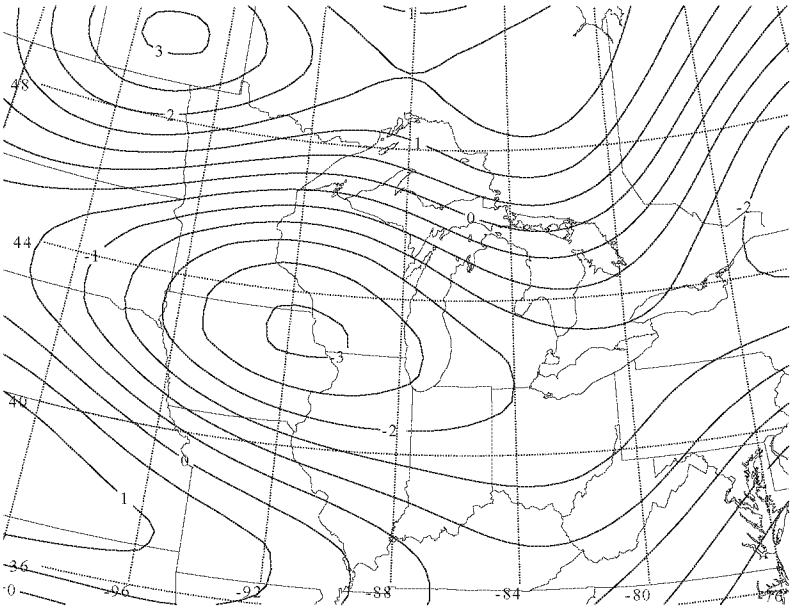

(d) Omega (solid in microbar/s).

Figure 14. Continued.

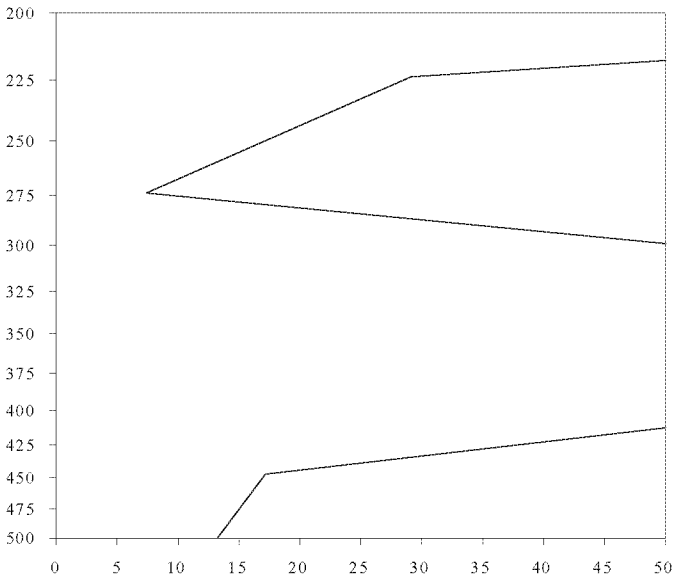

(e) Vertical profile of Richardson number.

Figure 14. Concluded.

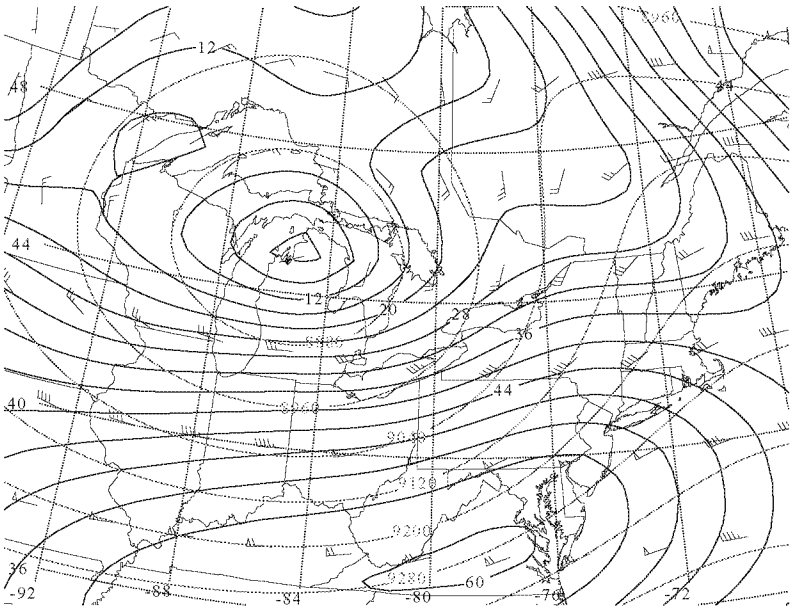

(a) Height (light solid in m), wind barbs (half barb = 5 ms^{-1}; full barb = 10 ms^{-1}; triangle = 50 ms^{-1}), and isotachs (dark solid in ms^{-1}).

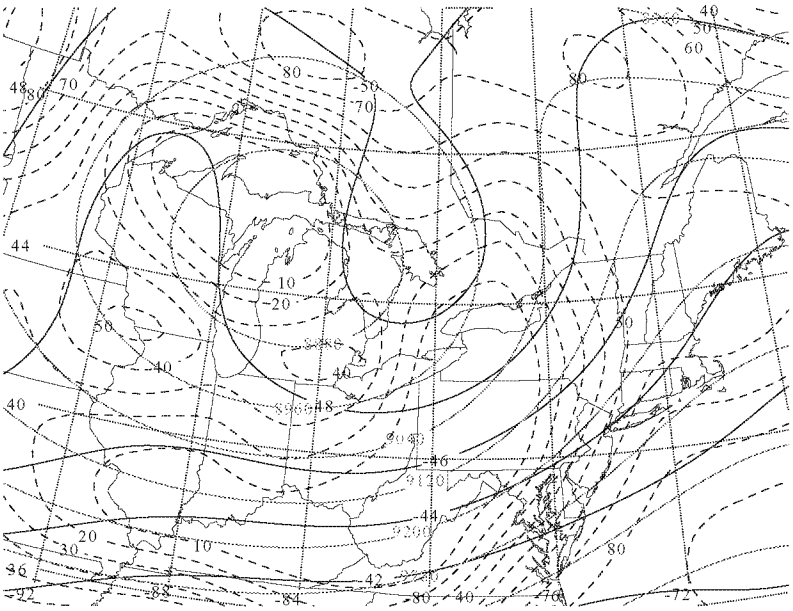

(b) Height (light solid in m), temperature (dark solid in C), and relative humidity (dashed in %).

Figure 15. 0000 UTC 24 March 1991 NCEP Reanalyses 300 mb.

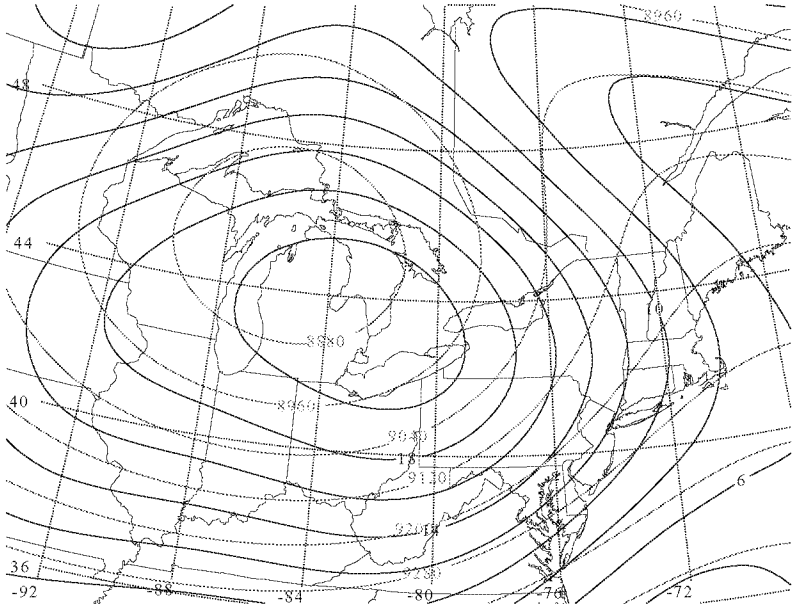

(c) Height (light solid in m) and absolute vorticity (dark solid in $s^{-1} \times 10^{-5}$).

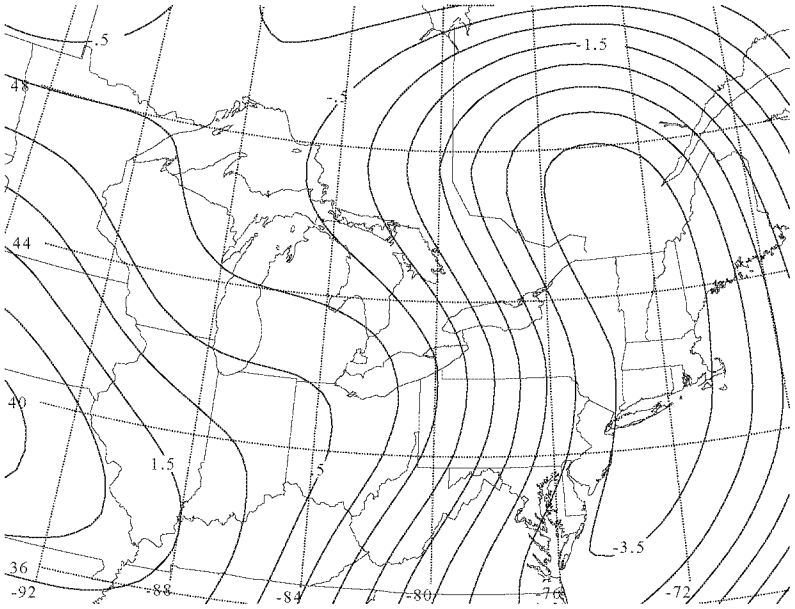

(d) Omega (solid in microbar/s).

Figure 15. Continued.

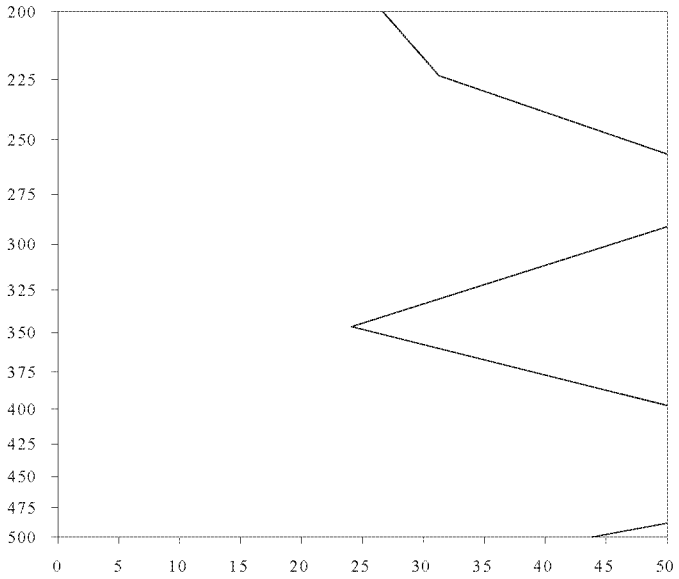

(e) Vertical profile of Richardson number.

Figure 15. Concluded.

REPORT DOCUMENTATION PAGE

Form Approved
OMB No. 0704-0188

1. REPORT DATE *(DD-MM-YYYY)*	2. REPORT TYPE	3. DATES COVERED *(From - To)*
08-2002	Contractor Report	

4. TITLE AND SUBTITLE

Characterizing the Severe Turbulence Environments Associated With Commercial Aviation Accidents

Part I: 44 Case Study Synoptic Observational Analyses

5a. CONTRACT NUMBER
NAS1-99074

5b. GRANT NUMBER

5c. PROGRAM ELEMENT NUMBER

6. AUTHOR(S)

Kaplan, Michael L.; Huffman, Allan W.; Lux, Kevin M.; Charney, Joseph J.; Riordan, Allan J.; and Lin, Yuh-Lang

5d. PROJECT NUMBER

5e. TASK NUMBER

5f. WORK UNIT NUMBER
728-40-30-01

7. PERFORMING ORGANIZATION NAME(S) AND ADDRESS(ES)

Research Triangle Institute
Research Triangle Park, NC 27709

8. PERFORMING ORGANIZATION REPORT NUMBER

9. SPONSORING/MONITORING AGENCY NAME(S) AND ADDRESS(ES)

National Aeronautics and Space Administration
Langley Research Center
Hampton, VA 23681-2199

10. SPONSOR/MONITOR'S ACRONYM(S)
NASA

11. SPONSOR/MONITOR'S REPORT NUMBER(S)
NASA/CR-2002-211918

12. DISTRIBUTION/AVAILABILITY STATEMENT

Unclassified - Unlimited
Subject Category 03
Availability: NASA CASI (301) 621-0390 Distribution: Standard

13. SUPPLEMENTARY NOTES

Kaplan, Huffman, Lux, Riordan, and Lin: North Carolina State Univ., Raleigh, NC. Charney: North Central Res. Stat., East Lansing, MI. Electronic version: http://techreports.larc.nasa.gov/ltrs/ or http://techreports.larc.nasa.gov/cgi-bin/NTRS
Langley Technical Monitor: Fred Proctor.

14. ABSTRACT

A 44 case study analysis of the large-scale atmospheric structure associated with development of accident-producing aircraft turbulence is described. Categorization is a function of the accident location, altitude, time of year, time of day, and the turbulence category, which classifies disturbances. National Centers for Environmental Prediction Reanalyses data sets and satellite imagery are employed to diag- nose synoptic scale predictor fields associated with the large-scale environment preceding severe turbulence. These analyses indicate a predominance of severe accident-producing turbulence within the entrance region of a jet stream at the synoptic scale. Typically, a flow curvature region is just upstream within the jet entrance region, convection is within 100 km of the accident, vertical motion is upward, absolute vorticity is low, vertical wind shear is increasing, and horizontal cold advection is substantial. The most consistent predictor is upstream flow curvature and nearby convection is the second most frequent predictor.

15. SUBJECT TERMS

Turbulence; Convection; Vorticity; Wind shear; Jet stream

16. SECURITY CLASSIFICATION OF:			17. LIMITATION OF ABSTRACT	18. NUMBER OF PAGES	19a. NAME OF RESPONSIBLE PERSON
a. REPORT	b. ABSTRACT	c. THIS PAGE			STI Help Desk (email: help@sti.nasa.gov)
					19b. TELEPHONE NUMBER *(Include area code)*
U	U	U	UU	57	(301) 621-0390